CARBON, OXYGEN AND HYDROGEN ISOTOPE FRACTIONATION IN MOLECULAR CLOUDS

A thesis submitted to the University of Manchester
for the degree of Master of Science
in the Faculty of Engineering and Physical Sciences

2013

By

Marion Mathelié-Guinlet

School of Physics and Astronomy

Contents

Word count: 21006

List of Tables

List of Figures

Abstract

The thesis "Carbon, oxygen, and hydrogen isotope fractionation in molecular clouds" is submitted in 2013 to the University of Manchester, by Marion Mathelié-Guinlet for the degree of master of science.

Comparison between observations and astrochemical models allows us to determine more precisely the physics and chemistry of an astronomical environment. One needs chemical tools to predict different parameters among which, the age and the underlying isotope ratios, to help observers focus on what should be the keys to deeply study this environment.

This thesis tries to figure out these chemical tools on large scale. It presents the upgrade of a chemical network, which includes the main isotopes of carbon (^{12}C, ^{13}C), oxygen (^{16}O, ^{18}O) and hydrogen (H, D).

The abundance ratios CS/SO and NH_3/SO appear to be good chemical clocks for early times (t $< 10^5$ years) whereas those of NH_3/HCN (NH_3/HNC) and NH_3/HCO^+ work well for later ages, as their temporal variations are sudden and strong over a defined period of time and for all densities between 10^3 and 10^7 cm^{-3}. Once dating the environment, other ratios are interesting to determine the carbon underlying ratio: HNC/HN^{13}C, $HCO^+/H^{13}CO^+$ and $CH^+/^{13}CH^+$. These tools have been applied to study a particular interstellar cloud : the cyanopolyyne peak of the Taurus Molecular Cloud TMC-1 is found to be around 2×10^5 years, has a density of 2×10^4 cm^{-3} and a carbon underlying ratio of 75.

Furthermore, the upgraded network is used to predict temporal and density variations over time of the isotopologues of HNCO, which is thought to trace either dense, far infrared or shocked regions. These strong temporal and density variations are compared with some basic molecules containing the main elements, such as HCO^+.

Declaration

I declare that no portion of the work referred to in this thesis has been submitted in support of an application for another degree or qualification of this or any other university or other institute of learning.

Marion Mathelié-Guinlet

University of Manchester

Jodrell Bank Center of Astrophysics

Oxford Road

Manchester

Copyright

restriction declarations deposited in the University Library, The University Librarys regulations (see http://www.manchester.ac.uk/ library/aboutus/regulations) and in The Universitys policy on presentation of Theses.

The author

In 2008, the author obtained a scientific Baccalauréat (equivalent to the A-level) with high honours in France. After two years of preparatory courses for the French "Grandes Ecoles", the author entered the School of General Engineering, Centrale Lyon. During the second year, she realized a research project with the Institute of Nanotechnologies of Lyon (INL) : she performed a design of experiment to synthesize monodisperse gold nanoparticles. As part of her third year in Centrale, she decided for a double master degree and began studying at the University of Manchester, in September. The results of her MSc by research in Astrophysics and Astronomy are presented in this thesis.

Acknowledgements

This research project was performed in the School of Physics and Astronomy, at the University of Manchester. So I would like to thank all the staff, students and academics who welcomed me and allowed me to work in remarkable conditions.

My thanks are particularly addressed to Andrew Markwick who supervised me throughout this year in my research. He shared with me his own experience and knowledge so that I did not feel lost in this "new world" which astrochemistry was for me. He answered all of my crazy questions with patience, details and instruction. Dr Markwick left me a lot of freedom in my work, allowing me to develop my own interpretations which were followed by constructive discussions. I really appreciated his guidance, his support over the year and the time he spent with me on this project, despite his busy schedule. Without his Perl scripts and his encouragements which were so invaluable, especially during the hard moments, this project might have failed.

I greatly thank Prof Gary Fuller, Matias Lackington, Catherine McGuire and Drs Adam Avison, Jaime Pineda, Alessio Traficante for their attentive ears and valuable advices during our weekly meetings. It was a real pleasure to hear about all their research studies. I was a bit confused sometimes but their explanations, precisions and interrogations make me jump joyfully in this extraordinary field.

I have also to say my gratitude to the whole Astrophysics team for sharing their passion for astronomy, either during internal seminars, JBCA colloquium or astro-ph sessions!

Last, but not least, I wish to thank my family without whom I would be lost. Their unconditional love, their presence and their encouragements over my studies (especially during the tough times away) have made me who I am now.

"Si quelqu'un aime une fleur qui n'existe qu'à un exemplaire dans les millions et les millions d'étoiles, ça suffit pour qu'il soit heureux quand il les regarde. Il se dit: 'Ma fleur est là quelque part . . . '."
Antoine de Saint Exupéry, *Le Petit Prince*

To my parents
To my twin sister
Always

Chapter 1

Introduction

1.1 General introduction

Astrochemistry overlaps several disciplines, mainly astronomy and physical chemistry. It studies the molecular composition of interstellar medium, planetary atmospheres and the evolution of matter in these environments. It has been an active field of research since the discovery in 1940 of some interstellar lines like CH, CH^+ and CN ([27]).

Observations of molecules enable us to constrain physical and chemical properties of media where they are found. Observational analysis is made in two ways :

- Studying spectra of rotational transitions observed in emission by telescopes sensitive to millimetre wavelengths,
- Studying spectra of vibrational transitions observed in absorption by telescopes sensitive to infrared wavelengths.

In addition to allow detection and identification of molecules, these spectra enable us to infer molecular abundances, densities and temperatures of astronomical

objects where molecules are found.

Because of the lack of spatial resolution, it is necessary to model molecular abundances in different astronomical objects. To do this, some astrochemical models are released which give the chemical network (all chemical reactions occurring) involved in a specific medium, and the rate of each chemical reaction. They allow astrophysicists to predict molecular abundances over time according to different physical parameters. The success of such a model is seen while comparing its results to the observed ones. Nowadays, there is no chemical model that can predict accurately all molecular abundances (only for some major elements). That is why, major challenges for astrochemistry are identifying sources of uncertainties in both observations and calculations, and determining key reactions that could explain everything.

1.2 The Interstellar Medium (ISM)

The role of astrochemistry is to detect and identify molecules in galaxies, stars and every other astronomical object. Between these objects the space is far from being empty : an interstellar medium (ISM) exists which consists of gas and solid matter. This diffuse medium plays a fundamental role in the evolution of matter. Stars are born there and when they die, they eject there some of the heavy elements produced by thermonuclear reactions. Thus, the ISM evolution is strongly related to stellar evolution. In a galaxy like the Milky Way, typically, one per cent of the ISM mass is formed by dust grains. This tiny part is responsible for lots of chemical and physical processes and for the extinction of stellar radiation.

1.2.1 Structure of the ISM

The ISM presents a wide range of physical conditions, originated from interactions with stellar or cosmic ray radiations and collisions. Therefore, it can be divided into sub-regions ([17]) according to the temperature T, molecular density n and state of hydrogen (the most abundant element in ISM) :

- **HII regions**. These ionised regions are hot and present a wide range of density. Traditional HII regions exhibit a temperature of about 10^4 K and can be dense, from 10^{-1} to 10^4 cm^{-3}. The coronal gas is warmer, T = 10^5 K - 10^6 K, and tenuous, n = 0.003 cm^{-3}.

- **HI regions**. These neutral regions are much less dense than traditional HII regions. According to temperature, there are divided in cool and warm sub-regions. Cool clouds are quite cold (T = 80 K) whereas warm gas is hot (T = 6000 K) but they are both tenuous (respectively n = 1 cm^{-3} and n = 0.05 - 2 cm^{-3}).

- **H_2 regions**. These molecular regions are cold. They are distinguished according to their density. Diffuse clouds (T = 40 - 80 K) are less dense (n = 100 cm^{-3}) than dense clouds (T = 10 - 50 K and n = 10^4 - 10^6 cm^{-3}).

Nowadays, about 150 species have been identified and H, N, C, O are the most abundant elements in these species. To understand how they are formed and destroyed, the chemistry of ISM has to be investigated.

1.2.2 The chemistry of the ISM

1.2.2.1 Rate of chemical reactions

Considering the low densities (compared with those on Earth), only two kind of processes can occur in the ISM :

- unimolecular reactions : a molecule reacts with a photon or a cosmic ray particle.
- bimolecular reactions : A + B $\xrightarrow{k}$ C + D

The rate at which the abundance of species A changes is given by :

$$r = \frac{dn(A)}{dt} = -k \times n(A) \times n(B) = -\frac{dn(C)}{dt} \tag{1.1}$$

where k is the rate constant and n(X) is the abundance of molecule X.

This equation can be generalised to any process (unimolecular or bimolecular) which involves formation and destruction of molecule A. The change in abundance of species i is :

$$r = [\sum_j k_j n(j) + \sum_{j,k} k_{jk} n(j) n(k)] - n(i)[\sum_j k_j + \sum_j k_{ij} n(j)] \tag{1.2}$$

where the first two sums correspond to the formation of species i and the second ones to its destruction.

Generally speaking, the rate constant depends on the temperature, following the Arrhenius equation :

$$k(T) = A \exp\left(\frac{-E_a(T)}{RT}\right) \tag{1.3}$$

where A is a constant, E_a the activation energy, T the temperature and R the gas constant.

However, in clouds, collisions between particles need to be added to the model, changing this temperature dependence ([26]) to :

$$k(T) = \alpha \left(\frac{T}{300}\right)^{\beta} \exp\left(\frac{-\gamma}{T}\right) \tag{1.4}$$

where α , β and γ are fitted experimental parameters.

1.2.2.2 Chemical reactions in the ISM

When two molecules collide in the gas phase of the ISM new species are formed. Depending on the nature of the reactants, chemical processes split in different categories. Table 1.1 sums up gas-phase reactions.

Type	Rate constant k	Example
Neutral - neutral	Eq (1.4)	$A + B \rightarrow C + D$
	4×10^{-11} cm^3 s^{-1}	
Ion - molecular	Eq (1.4)	$AB + C^+ \rightarrow BC^+ + A$
	2×10^{-9} cm^3 s^{-1}	
Photoreactions	$k(T) = \alpha \exp(-\gamma A_v)$ [26]	$AB + h\nu \rightarrow A + B$
	10^{-9} s^{-1}	$A + h\nu \rightarrow A^+ + e^-$
Cosmic ray ionisation	$k(T) = \alpha$ [26]	$A + c.r \rightarrow A^+ + e^- + c.r$
Recombination	Eq (1.4)	$A^+ + e^- \rightarrow A + h\nu$
	10^{-7} cm^3 s^{-1}	$AB^+ + e^- \rightarrow A + B$
Charge transfer	Eq (1.4)	$AB + C^+ \rightarrow AB^+ + C$
	10^{-9} cm^3 s^{-1}	
Radiative association	Eq (1.4)	$A + B \rightarrow AB + h\nu$
	reaction specific	

Table 1.1: Types of gas phase reactions ([17]).

However, gas-phase chemistry is not sufficient to explain observed abundances of many species in the ISM. One of the most striking examples is molecular hydrogen. It requires not only two atomic hydrogens but also a third body to be formed :

$H + H \rightarrow H_2$. Dust grains provide a surface where many processes can occur even if their probabilities are not completely known yet ([17]):

- **Accretion** : at temperature of a molecular cloud ($\approx$ 10 K), the probability for a species to remain bound to the surface is close to 1 except for atomic H (the probability is lower and decreases when temperature gets higher).
- **Desorption** : when grains receive energy from thermal fluctuations (absorption of UV photons, heat of reactions ...), radiations or chemical reactions, the release of a species can occur in the gas phase.
- **Contact between two species**. Either mobile species move across dust surface to react with stationary species,or accreted species bond directly to stationary ones. The first process is known as the Langmuir Hinshelwood mechanism and the second as the Eley Rideal mechanism.

1.2.3 Molecular excitation and radiative transfer equation

1.2.3.1 Molecular excitation

Consider a system of two levels u and l, with $E_u > E_l$ and populated respectively by n_u and n_l. The equilibrium state gives :

$$\frac{dn_u}{dt} = n_l(B_{lu}\overline{J} + c_{lu}) - n_u(A_{ul} + B_{ul}\overline{J} + c_{ul}) = 0 \tag{1.5}$$

where :

- B_{lu} and B_{ul} are Einstein coefficients : they represent the rate coefficients for respectively stimulated absorption and stimulated emission,
- A_{ul} is another Einstein coefficient : it is the rate coefficient for spontaneous decay,

- c_{ul} and c_{lu} are the rate coefficients for respectively collisional de-excitation and excitation,

- $\overline{J}$ is the mean intensity of the radiation field, defined by

$$\overline{J} = \frac{1}{4\pi} \int \int I_\nu \Phi_\nu d\Omega d\nu. \tag{1.6}$$

where Φ_ν is the line profile and I_ν is the specific intensity :

$$I_\nu = \frac{dE}{dt dA d\nu d\Omega}. \tag{1.7}$$

If the level populations are Boltzmann distributed, then an excitation temperature T_{ul} can be defined :

$$\frac{n_u}{n_l} = \frac{g_u}{g_l} \exp\left(-\frac{h\nu_{ul}}{kT_{ul}}\right) \tag{1.8}$$

where g_u and g_l are the level statistical weights, ν_{ul} the frequency of the downward transition and k the Boltzmann constant.

If collisional processes are dominant, then the excitation temperature is the kinetic temperature of the gas. Thus, it is equal for each transition. On the other hand, if radiative processes are dominant, then the excitation temperature tends to be the temperature of the blackbody radiation :

$$I_\nu = B_\nu = \frac{2h(\nu)^3}{c^2} \times \frac{1}{\exp\left(\frac{h\nu}{kT}\right) - 1}. \tag{1.9}$$

The critical density is defined as the H_2 density at which collisional processes equal radiative ones :

$$n^*_{H_2} = \frac{A_{ul}}{C_{ul}}. \tag{1.10}$$

where $C_{ul} = \frac{c_{ul}}{n_{H_2}}$ is the coefficient for downward collisions.

1.2.3.2 Radiative transfer

When radiation propagates through the interstellar medium, it can interact with matter which can either absorb or emit radiation. Therefore, the intensity (defined in equation 1.7) will change with distance. This is known as the radiative transfer equation :

$$\frac{dI_\nu}{ds} = -\kappa_\nu I_\nu + j_\nu. \tag{1.11}$$

where s is the distance, κ_ν the absorption coefficient and j_ν the emission coefficient.

At this point, it is usual to introduce the optical depth τ_ν, defined as :

$$\tau_\nu = \int \kappa_\nu ds. \tag{1.12}$$

The absorption coefficient can be expressed in terms of the Einstein B coefficients, previously defined (see equation 1.5). Thus, the optical depth of an upper lower transition can be defined as :

$$\tau_\nu = \frac{c^2}{8\pi\nu_{ul}^2} A_{ul} N_u \left(\exp\left(\frac{h\nu_{ul}}{kT_{ul}}\right) - 1\right) \Phi(\nu). \tag{1.13}$$

where $N_u = \int n_u ds$ is the column density of the upper level. The temperature is assumed not to depend on the distance s.

Then assuming a Boltzmann distribution of populations, the total column density N of molecules, applying only in LTE conditions, is given by :

$$N = \sum N_i = \frac{N_0}{g_0} \exp\left(\frac{E_0}{kT}\right) Q(T). \tag{1.14}$$

where the subscript 0 refers to the ground state. Q(T) is the partition function

which depends only on the molecule constants and temperature :

$$Q(T) = \sum g_i \exp\left(\frac{-E_i}{kT}\right). \tag{1.15}$$

1.3 Astrochemical models

The purpose of astrochemical models is to reproduce the observed abundances for all species detected in the ISM. The most simple models consider only gas-phase chemistry, except for the formation of H_2 which occurs on dust grains. Such models require the knowledge of physical and chemical conditions. As a consequence, a specific model assumes values for the gas temperature T, the gas density n, the ionisation rate ζ, the visual extinction A_v and the initial abundances of each and every species. In addition, a model provides the chemical network along with the rate constant of each reaction of this network.

It is obvious that all these parameters are not accurately known. Thus, to run an astrochemical model, some assumptions are made, notably for reaction rate and chemical network. Indeed, for some reactions the rate coefficient is only known theoretically whereas for others, many experimental results are available. The choice of Q has to be made on whether to take experimental or theoretical rates. Moreover, in order to simplify the model, some reactions are neglected because it is thought that they won't participate much in the chemistry of a specific astronomical object.

When the model is run, it solves a system of Ordinary Differential Equations (ODEs). We assume that the studied molecular cloud reaches a state of equilibrium, implying that the abundance of each species does not vary much in time. This approximation is known as the steady state approximation and equation 1.2 gives :

$$\frac{dn(i)}{dt} = [\sum_j k_j n(j) + \sum_{j,k} k_{jk} n(j) n(k)] - n(i)[\sum_j k_j + \sum_j k_{ij} n(j)] = 0 \tag{1.16}$$

For each species, i, such equations can be written. Considering the whole chemical network, these ODEs are coupled in a way that only computer power can solve the problem. Finally, when the program is run, it provides an output concerning the time dependence of species abundances (it is implicit thereafter that the abundance is relative to H_2). Then, these results are compared with observations. Some parameters are experimentally fitted to match the latter and so on ... to obtain a model that can predict observations with great accuracy. However, it is important not to forget the grain chemistry as it might be the point explaining all failures until now in running models.

1.4 Chemical fractionation

1.4.1 Deuterium fractionation

Since many deuterated species (HD, H_2D^+, DCN, N_2D^+ ...) have now been observed in the ISM, deuterium chemistry is widely discussed and attention has been paid to its isotopic fractionation. The elemental D to H ratio is thought to be approximately 10^{-5} ([33], [30], [20]). One could say that the abundance ratio between deuterated and normal species should reflect this underlying ratio. However, it is far from being true. There are some discrepancies in the deuterium to hydrogen ratio itself, implying that chemical and/or physical processes affect deuterium abundance :

- Radiation pressure mechanisms;
- Shielding of H_2 from photodissociation;
- Chemical fractionation;
- Collisions with hydrogen or other species.

Figure 1.1 shows the inhomogeneous distribution of the D to H ratio. In 1981, only a small sample was available, of nearby stars and in front of more distant early type stars ([2]). More recently, Linsky et al, based on spectra of the *FUSE* mission, reported the same inhomogeneity in the D to H ratio for many lines of sight towards the Milky Way and beyond. They stated that three different behaviour occur depending on the total column density of neutral hydrogen. They also developped a model where they correlated the (D/H) variations with the depletion of deuterium onto dust grains which leads to lower ratios in the gas phase. Similarly, the low values of $(D/H)_{gas}$ seem to correlate well with the depletion of iron and silicon.

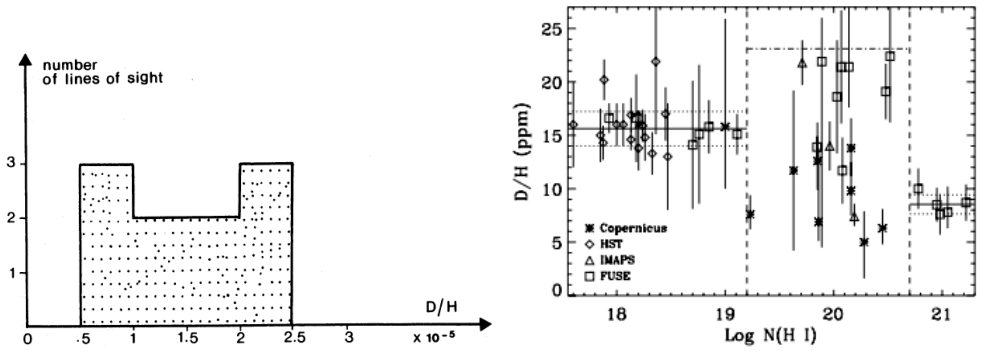

(a) Histogram of the D/H ratios ([2]).

(b) Plot of the D/H ratios against the hydrogen column density ([20]).

Figure 1.1: The inhomogeneous distribution of the deuterium to hydrogen ratio.

Roberts et al even predicted that in dense and highly depleted regions, the atomic ratio [D]/[H] could be greater than 0.3, due to the high deuterium fractionation occurring when species like HD_2^+ and D_3^+ are included in models. Though, they predicted a limit on the deuterium enrichment : 0.25 - 0.4 for singly deuterated moleculesm for highly depleted regions, which is not always confirmed by observations ([36]).

Deuterium enhancement depends significantly on temperature and ionization rate. Basically, deuterium can be fractionated into different species via three ions, H_2D^+, CH_2D^+ and C_2HD^+. At low temperatures, the most prevalent deuterium fractionation reaction is :

$$H_3^+ + HD \xrightarrow{k} H_2D^+ + H_2$$

The reverse reaction has an energy barrier of 270 K. At small temperatures, H_2D^+ persists and drives the gas deuteration whereas at higher temperatures, the reverse reaction occurs and destroys H_2D^+. However, deuteration still persists since other reactions like

$$CH_3^+ + HD \rightarrow CH_2D^+ + H_2 + \Delta E = 370 \text{ K}$$

$$C_2H_2^+ + HD \rightarrow C_2HD^+ + H_2 + \Delta E = 550 \text{ K}$$

produce enough CH_2D^+ and C_2HD^+ to maintain an enhancement in deuterated species. As temperature increases, fractionation due to reaction involving H_2D^+ falls while that caused by CH_2D^+ and C_2HD^+ rises ([29], [23]). This temperature dependence partly explains the difference in observed deuterated species ratios.

Millar, Bennett and Herbst performed an extensive model including deuterium ([29]). They emphasized another important aspect that the abundance of deuterated species strongly depends on time. Most of the calculations use steady state conditions (t = 10^8 years) whereas it has been proved that observations are best fitted with early time conditions (t $\leq 3.10^5$ years). A striking example is that of the ratio between DCO^+ and HCO^+ that is predicted to be one third of the one between H_2D^+ and H_3^+ ([29]). This holds whatever the time is, at 10 K, but fails in early times when the temperature increases(see figure 1.2). Actually, at early times, the abundances of many complex molecules reach a maximum, then they decrease and remain constant at steady state. The large ratio for DCO^+ can be explained by the following reaction involving an hydrocarbon which follows the previous criterion :

$$CH_4D^+ + CO \rightarrow DCO^+ + CH_4$$

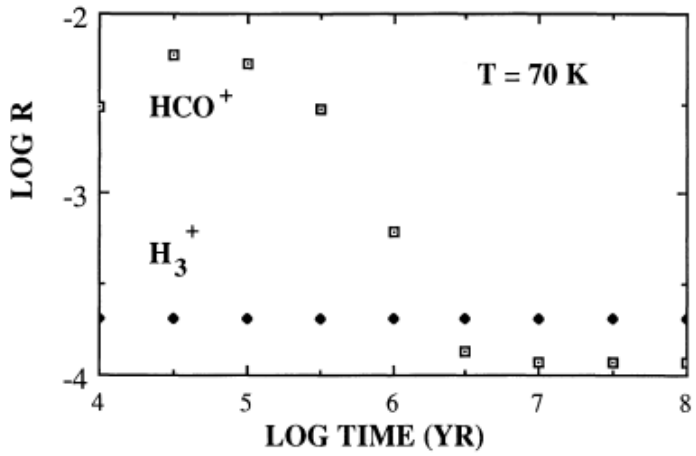

Figure 1.2: Time dependence of the ratio, R, between deuterated and normal isotope species for HCO^+ and H_3^+ ([29]).

Deuterated and multi-deuterated species have been observed in a lot of different environments and are quite well studied in astrochemical models. Table 1.2 presents some of the most studied molecules with their ratio with respect to the hydrogen-bearing species.

Object	Temperature	$\frac{[DCO^+]}{[HCO^+]}$	$\frac{[DCN]}{[HCN]}$	$\frac{[DNC]}{[HNC]}$	$\frac{[DC_3N]}{[HC_3N]}$
TMC 1	10	0.015 [11]	0.023 [55]	0.015 [11]	0.015 [45]
Orion	70	0.002 [34]	0.006 [55]	0.01 [1]	
TW Hydrae		0.017 [32]	0.017 [32]		

Table 1.2: Ratios of some deuterated species in different environments.

The chemical fractionation effects for isotopes of C and O are also significant even though they are much smaller than for H. Besides, even though many ^{13}C and ^{18}O bearing molecules have been detected, much less attention has been paid for their study.

1.4.2 Carbon isotope fractionation

The $^{13}C/^{12}C$ ratio is of great importance for the determination of nuclear processing products in the ISM. Observations of many species involving carbon, mainly carbon monoxide CO, has helped its study. It was found that this ratio is greater than the terrestrial one, which is 1/90. Depending on where observations are made, it lies in a quite wide range, between 1/90 and 1/40. Chemical fractionation might explain this anomaly.

The most important fractionation reaction for carbon is an isotopic exchange reaction ([51]) :

$$^{13}C^+ + {}^{12}CO \xrightarrow{k} {}^{13}CO + {}^{12}C^+ + \Delta E$$

where $k = 2.10^{-10}$ cm^3 s^{-1} and the energy barrier is $\frac{\Delta E}{k} = 35$ K.

This small energy difference makes the forward reaction more efficient at low temperatures. Thus ^{13}C shifts into ^{13}CO, decreasing the abundance ratio of ^{12}CO to ^{13}CO, while the one of $^{12}C^+$ to $^{13}C^+$ increases. The reverse reaction, more probable at higher temperatures, has a rate coefficient of $k_r = k \times \exp(-35/T)$. Few years after Watson et al., Smith and Adams performed a more detailed study (between 80 and 500 K) on the strong temperature dependence of these two rate coefficients ([42]).

Langer et al were the first to perform numerical calculations with a time-dependent chemistry model including isotopes ([19]). They were able to distinguish three groups in the behaviour of carbon isotope ratios : CO, HCO^+ and the "carbon isotope pool" with the remaining carbon-bearing species (CS, H_2CO, HCN ...). Ratios of such species can be bracketed by :

$$\frac{^{12}CO}{^{13}CO} \leq \frac{^{12}C}{^{13}C} \leq \left(\frac{H_2{}^{12}CO}{H_2{}^{13}CO}, \frac{^{12}CS}{^{13}CS}, \ldots\right)$$

The ratio concerning HCO^+ is not correlated to the other ones since this molecule can be produced both from CO and species from the "pool". Thus, it is a mix between the two other groups.

The enhancement in $^{13}CO/^{12}CO$ varies with physical conditions. It strongly depends on the position in the cloud. For instance, in outer parts of dark clouds, ^{13}CO abundance is higher by a factor 3-7 than in central positions ([18]). Also, even fractionation of CO occurs over a large range of densities and temperatures, it is higher for low densities, low temperatures and high metal abundance (see figure 1.3). Indeed, in these conditions, fractionation of CO is larger because the electron fraction is larger, allowing fractionation to compete with usual CO production pathways ([19]).

Isotope fractionation for all the other species, through isotopic exchange, seems unimportant since it produces chemically distinct species from reactants. In this case the abundance of ^{12}C is enhanced whatever conditions are. The only exception could be HCO^+. Indeed, as it could be produced both from CO and other carbon species, both twelve and thirteen carbon abundances can be enhanced. With increasing temperature, isotopic fractionation for these species decreases. Thus, the highest isotopic carbon ratios are reached for the lowest temperatures and for quite low densities (10^3 - 10^4 cm^{-3}) ([19])(see figure 1.3).

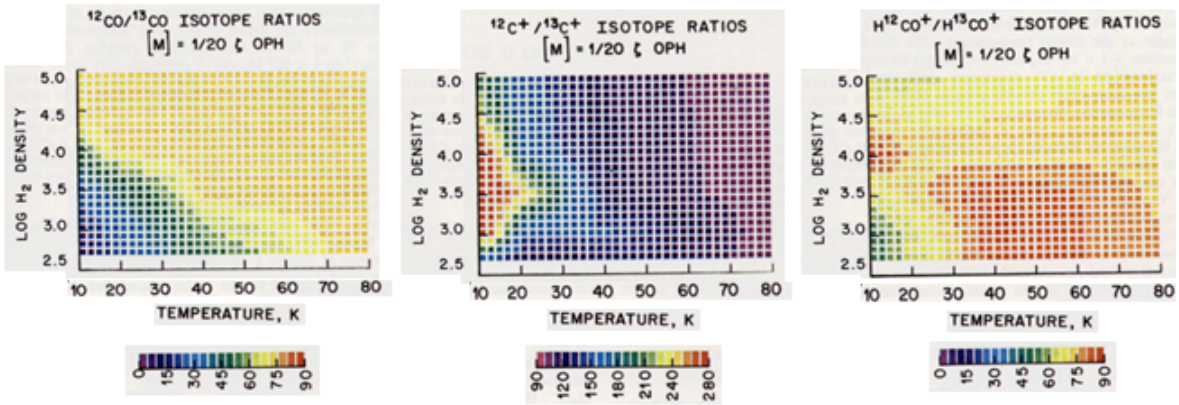

Figure 1.3: Isotopic ratios as a function of temperature and density ([19]).

In addition, all these isotopic ratios depend significantly on time. Up to t $\approx 10^6$ years, ratios show strong variations (see figure 1.4) due to all the reactions involving the key species of carbon isotope fractionation, such as C^+ and CO. After this time, steady state is established and ratios remain barely constant ([19]).

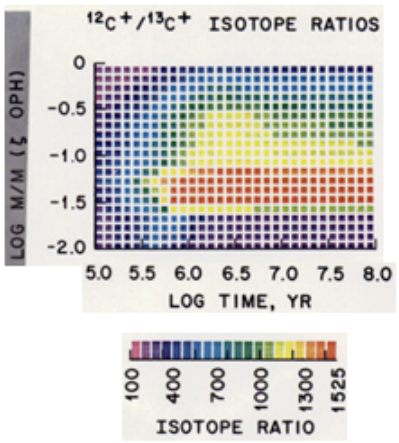

Figure 1.4: Isotopic ratio $^{12}C^+/^{13}C^+$ as a function of metal abundance and time ([19]).

Table 1.3 presents some of the most studied carbon isotopic bearing molecules.

Object	$\frac{[^{12}C]}{[^{13}C]}$	$\frac{[^{12}C^{18}O]}{[^{13}C^{18}O]}$	$\frac{[^{12}CO]}{[^{13}CO]}$	$\frac{[H_2{}^{12}CO]}{[H_2{}^{13}CO]}$	$\frac{[H^{12}CO^+]}{[H^{13}CO^+]}$	Reference
Terrestrial	90					
Dark cloud	80-90	50-80				[18]
Diffuse cloud			15-170			[21]
Protoplanetary disks	45-110		25-77	60-100		[54]
Galactic centre	25	24.5		22.5	23.5	[19]
Galactic ring	100	81		62		[19]

Table 1.3: Ratios of some carbon isotopologues in different environments.

1.4.3 Oxygen isotope fractionation

Oxygen isotope transfer ([19]) is accomplished by, for example,

$$HC^{16}O^{+} + C^{18}O \rightarrow HC^{18}O^{+} + C^{16}O + \Delta E$$

where -ΔE = 1.2 meV (14 K).

In opposition to carbon isotope fractionation, that of oxygen is not significant at any physical conditions because only few reactions can produce efficiently atomic isotope oxygen. Because of small rate coefficients and activation energy barriers, those reactions are unlikely to lead to oxygen fractionation. The only exception is HCO^{+} where ^{18}O can be enhanced at very low temperatures. Thus, the oxygen isotope ratios reflect more nuclear processing than chemical fractionation. Table 1.4 presents some of the most studied oxygen isotopic bearing molecules.

Object	$\frac{[^{17}O]}{[^{18}O]}$	$\frac{[^{16}O]}{[^{18}O]}$	Reference
Terrestrial		490	
Dark cloud	2.6	250	[18]
Galactic centre		350	[19]
Galactic ring		700	[19]

Table 1.4: Ratios of some oxygen isotopologues in different environments.

1.5 Thesis overview

The major aim of this work is to find a general scheme that could help observers to figure out the carbon underlying ratio in a specific environment. This ratio is the initial value of $^{12}C/^{13}C$ in the interstellar medium; abundances and isotopologic ratios for other carbon-bearing species depend on this value. To a minor extent, the physical conditions affecting formation and destruction of HNCO, which is thought

to be a cold dense region tracer, are investigated. Some studies were performed for particular molecules but they never included at the same time carbon, oxygen and hydrogen isotopes. Consequently, the focus of the project is to upgrade a chemical network with ^{13}C, ^{18}O and D that could be used along with a previously developed chemical model to investigate any molecule at any timescale, in various physical conditions.

The basic knowledge of astrochemistry from its constituents both in gas and grain phases to the role of the main isotopes of carbon, oxygen and hydrogen has been now reviewed. The rest of this thesis is divided up into five chapters. Chapter 2 describes the chemical network and model developed in this work from the initial elements required to how it was obtained. Chapter 3 focuses on the results obtained for isocyanic acid and compare them with some other fundamental species. Density and time dependences are there described for HNCO and its isotopologues. The main result of this project is treated in Chapter 4 : the scheme developed to find the age of the observed environment and subsequently the carbon underlying ratio is discussed. Then, it is applied to the Taurus Molecular Cloud TMC-1 in chapter 5. Finally, chapter 6 concludes with a summary of the obtained results and possible future works.

Chapter 2

The chemical model

The purpose of an astrochemical model is to describe the temporal variations of various species in an astronomical environment. As discussed in section 1.3 running a model requires the knowledge of several parameters, including a chemical network which sets all the reactions for formation and destruction of each and every species.

Thereafter, if no superscript is indicated then the molecule contains the main isotope (either ^{12}C or ^{16}O). In addition, when analysis is made, the temperature has been fixed to 10 K if not otherwise indicated.

2.1 The reaction network

2.1.1 Structure

The reaction network contains essential information for calculations of rate coefficients which allow us to determine the abundance (relative to molecular hydrogen) of species at every timescale, temperature and density. Basically, it includes the following parameters :

- Type of reaction : depending on the nature of reactants, reactions are subdivided into categories;
- Reactants (normally 2) and products (usually 2, but there can be 3 or 4);
- α, β and γ, constants which allow us to calculate the rate coefficients;
- Temperature ranges in which the rate coefficient is valid.

For instance, the Charge Exchange reaction between C^+ and C_2H_4 is written :

$$148 : CE : C^+ : C_2H_4 : C_2H_4^+ : C : : : 1 : 1.70e\text{-}11 : 0.00 : 0.0 : 10 : 41000 : \text{reference}$$

148 is the number of the reaction which has an alpha constant of 1.7×10^{-11} (here equals the rate coefficient as beta and gamma are equal to zero), valid between 10 K and 41000 K.

For more information on the structure of this reaction network, see the UMIST database for astrochemistry ([26]).

2.1.2 Fractionation of the reaction network

A chemical reaction network has been constructed with carbon (^{12}C, ^{13}C), oxygen (^{16}O, ^{18}O) and hydrogen (H, D) isotopes. It is based on the fifth release of the UMIST Database for Astrochemistry which contains 6173 gas-phase reactions and involves 467 species ([26]). A program has been developed to expand this "start network", including isotopes previously mentioned. It ended up with 97301 reactions and 1955 species. In a first attempt gas-grain interactions are not considered, except for the formation of H_2 on grain surfaces. But it can be easily treated in the model by adding an extra term of destruction on grain surfaces in the ODEs file.

Firstly, we have deleted in the "start network" all species involving strictly more than three carbons, phosphorus and chlorine because they do not make a big difference in temporal variations of abundances of most other species.

Secondly, based on this reduced network, isotopes are included in the following order : carbon, oxygen and hydrogen. Normally, when only main isotopes are considered, atoms are indistinguishable in a molecule : it is not possible to state which atoms are linked together. However, including the different isotopes changes this fact (hereafter, the subscript for the main isotope is omitted). For instance,

$$H^- + C_2 \rightarrow C_2H + e^-$$

splits into

$$H^- + C^{13}C \rightarrow C^{13}CH + e^-$$

$$H^- + C^{13}C \rightarrow {}^{13}CCH + e^-$$

where the two carbons are now distinguishable.

But if an isotope can be placed in different positions or if molecules are much more complex, this procedure becomes complicated. In addition, with thousands of reactions in the network, it is not possible to decide by hand whether isotopologic reactions are allowed or forbidden. It is necessary to develop a program that can implement automatically the reaction network by including isotopologues of each species. This procedure is based on three steps, which will be described below.

2.1.2.1 Inclusion of isotopologues

The hardest part in updating the reaction network lies in including ^{13}C species. Indeed, as many carbon-bearing species are carbon-chains, it is difficult to account both for the existence of different isotopomers and the veracity of an isotopologic reaction. Different cases have been determined, depending on the nature of species and reactions to end up, as much as possible, with the right isotopologic reactions. Reactions involving :

- only one carbon per reactant and product channels,
- symmetrical species with only two carbons on both reactant and product sides,
- a charge transfer or a mutual neutralization,
- the same preservable carbon chain on both reactant and product sides

generate only one possibility of replacing the main isotope.
For instance,

$$C^- + O \rightarrow CO + e^-$$

splits into only one isotopic reaction :

$$^{13}C^- + O \rightarrow {}^{13}CO + e^-$$

For other reactions, things are more complicated. As much as possible, functional groups are preserved on both reactant and product sides.

Doing that, we do not consider multiple isotope species (only one ^{13}C can replace one ^{12}C) but we distinguish between different isotopomers : mainly, in carbon-chains, carbons are not equivalent so every position in which the isotope can be placed must be considered. For oxygen and hydrogen, the procedure is simpler since chains and

symmetry are not real concerns. Consequently, working out which reactions are considered to be right is easier.

For deuteration, the only thing that matters is the number of H-group per species. Firstly, the program tries to categorise the different reactions, depending on this number but also on the nature of species and/or reaction itself. Is there only one H-group in both reactants and products? Is the reaction a charge transfer? Is it a proton transfer between a reactant and a product? Are there more than one H-group per side (reactant/product)? In this case, is there a break or a binding between H-groups? Is there specific group in the reaction, such as CH_3 or HNC/HCN? Once, all reactions have been analysed, the program applies different rules according to categories. If the reaction belongs to the first category, then a brute deuteration is enough. If it is a charge transfer, one has to be careful to preserve the form : only a plus or minus sign distinguishes reactants and products, so the same species concatenated with +/- are found in both side. Things become much more complicated when several H-groups exist. If it is a proton/deuteron transfer, then the allowed reactions are the ones which transfer the same number of atoms as in the original reaction. For instance, by brute deuteration, the reaction

$$H + NH_3 \rightarrow NH_2 + H_2$$

splits into

$$D + NH_3 \rightarrow NHD + H_2$$

$$D + NH_3 \rightarrow NH_2 + HD$$

$$H + NH_2D \rightarrow NHD + H_2$$

$$H + NH_2D \rightarrow NH_2 + HD$$

However, the first isotopologic reaction is assumed to be wrong as it transfers two atoms instead of one. It is worth noting the specific reactions involving $HCNH^+$ which can originate from or produce HCN and HNC. When including deuterium, the same phenomena occurs : $DCNH^+$ (respectively $HCND^+$) can be associated both with DCN and HNC (respectively HCN and DNC). If reactions are not part of any category, then all deuteration options are left.

Finally, including oxygen isotopes is easier since there are no species in the chemical network with more than one O-group. The trickiest cases are the split of an O_2 into two different species or the binding of two oxygen atoms into O_2. Thus, the same rules apply even though the majority of reactions just need the "brute way".

2.1.2.2 Scale of reaction rates

By introducing isotopologues in the chemical network, the whole chemistry changes. So isotopologic reaction rates need to be scaled. For the main reactions, they are known either by theory or observation whereas, for the isotopologic ones, they are undetermined. Even branching ratios between these two kind of reactions are unknown. Thus, strong assumptions are made. First, the rate coefficient is unchanged between reactions involving (i) the main isotope and (ii) the minor isotope. Second, if several isotopologic reactions exist, all branches have equal probabilities. As a consequence, if some reactions (resulting from the same initial reaction) have the same reactants but different product channels, their rate is equal to the initial rate divided by the number of product branches. For example, the reaction

$$C_2 + O \xrightarrow{k} CO + {}^{12}C$$

splits into

$$C^{13}C + O \xrightarrow{k_1} CO + {}^{13}C$$

$$C^{13}C + O \xrightarrow{k_2} {}^{13}CO + C$$

If we apply the previous assumptions, then the following relationships exist between the three coefficient rates :

$$k = k_1 + k_2$$

$$k_1 = k_2 = \frac{k}{2}$$

Concretely, the program searches how many reactions have the same reactants. When, the chemical network is truly updated with isotopologues, this number is also the number of places where the isotope can go in the reaction. Thus, knowing which are the main reaction and its rate, the resulting isotopologic reactions are scaled by this number.

Here is a final example where ^{13}C, ^{18}O and D are included. The reaction

$$C^- + OH \xrightarrow{k} HCO + e^-$$

splits into seven isotopic reactions :

$$C^- + OD \rightarrow DCO + e^-$$

$$C^- + {}^{18}OH \rightarrow HC^{18}O + e^-$$

$$C^- + {}^{18}OD \rightarrow DC^{18}O + e^-$$

$${}^{13}C^- + OH \rightarrow H{}^{13}CO + e^-$$

$${}^{13}C^- + OD \rightarrow D{}^{13}CO + e^-$$

$$^{13}C^- + {}^{18}OH \rightarrow H^{13}C^{18}O + e^-$$

$$^{13}C^- + {}^{18}OD \rightarrow D^{13}C^{18}O + e^-$$

Using the previous assumptions on branching ratio, all these reactions have the same rate coefficient, k.

2.1.2.3 Inclusion of fractionation reactions

Finally, we include fractionation gas-phase reactions, listed in table 2.1, taken from Langer et al ([19]). They are not present in the initial reduced network since when only the main isotope is considered, reactants and products are identical in these specific reactions.

2.2 Initial chemistry

In addition to a reaction network, the model needs the knowledge of what species are involved in reactions. A file lists all of them , along with their initial abundance and their mass. Except for hydrogen, which is initially present in molecular form (H_2), the initial chemical composition is assumed to be atomic. Also, C is assumed to be neutral instead of ionized, like in the UMIST database (2012), as it will not make any big differences : the present conclusions (trends, shapes and main reactions involved in HNCO and its isotopologues formation (see section 3.2)) are not affected by this state. Table 2.2 presents the initial chemistry for species with non zero initial abundances, based on the last release of the UMIST database for astrochemistry ([26]).

The total initial gas phase abundance of carbon is assumed to be less than the oxygen one, which is consistent with the fact that carbon is less abundant through

the interstellar medium and can be embedded in grains.

The values of the initial isotopic ratios are not straightforward. Except when mentioned, the following ratios are adopted : $HD/H_2 = 3 \times 10^{-5}$ ([20]), $^{12}C/^{13}C = 75$ and $^{16}O/^{18}O = 500$ ([52]). They are closed to observational values : for the deuterium ratio, many lines of sight are involved to do this average whereas for the carbon and oxygen ratios, only three clouds were considered. These values were also used in theoretical models ([29], [19]).

2.3 The chemical model

To determine the abundance of a species, its total rate of change is calculated. It is the result of the difference between the formation and destruction rates. Each of this term are worked out by analysing the reaction network according to equation 1.16. Consequently, an ordinary differential equation (ODE) is associated with each species. Those ODEs are coupled, since abundance of a particular species depends on formation and destruction rates of other species. The Double precision Variable coefficient Ordinary Differential Equation solver method (DVODE) solves numerically the system of ODEs obtained for the whole network. One of the way to solve this system is to assume the steady state approximation which implies that the rate of each reaction is equal to zero. By doing so, abundances could be deduced. Otherwise, abundances are worked out less easily.

Inside the main program, rate coefficients are calculated depending on the temperature chosen to run the model (see equation 1.4). Physical parameters (temperature, density, cosmic ray ionisation rate and visual extinction) are not fixed, they can be changed inside this program to study different environments.

The model output provides the abundance of each species at several time scales. The model starts at t = 0 and stops at t = 2×10^8 years, where the chemical

evolution is assumed to end.

Figure 2.1 is a scheme of the chemical model used for this project.

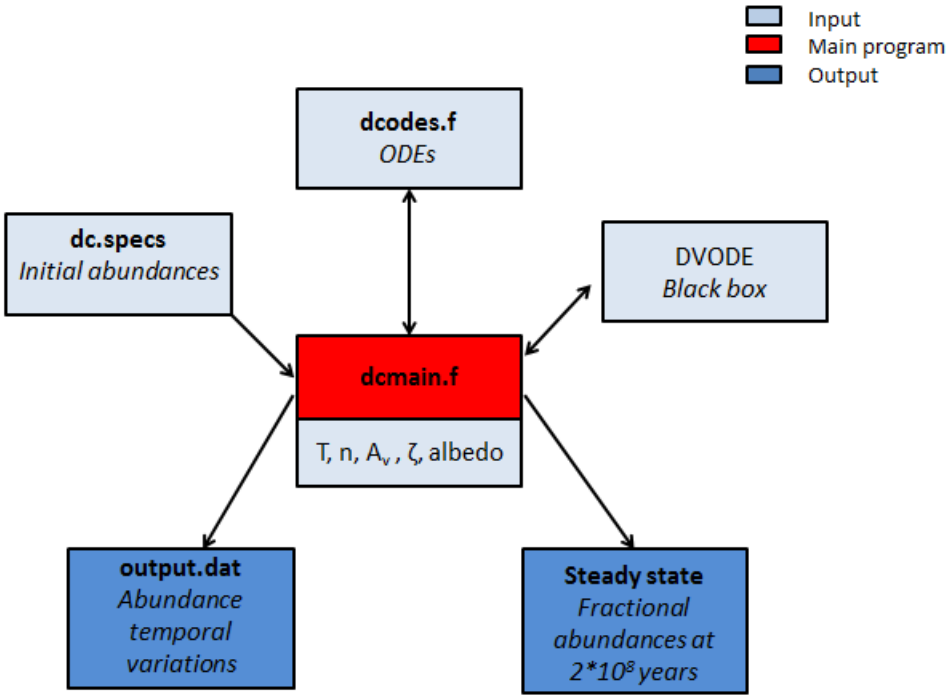

Figure 2.1: Scheme of the chemical model.

Reactions	Rate constant k	
	α	β
$H_3^+ + HD \rightarrow H_2D^+ + H_2$	1.7(-9)	
$H_2D^+ + H_2 \rightarrow H_3^+ + HD$	3.6(-18)	
$CH_3^+ + HD \rightarrow CH_2D^+ + H2$	1.3(-9)	
$CH_2D^+ + H_2 \rightarrow CH_3^+ + HD$	8.7(-10)	370.0
$C_2H_2^+ + HD \rightarrow C_2HD^+ + H2$	1.0(-9)	
$C_2HD^+ + H_2 \rightarrow C_2H_2^+ + HD$	2.5(-9)	550.0
$^{13}C^+ + CO \rightarrow C^+ + {}^{13}CO$	1.34(-9)	
$C^+ + {}^{13}CO \rightarrow {}^{13}C^+ + CO$	0.4(-10)	
$^{13}C^+ + C^{18}O \rightarrow C^+ + {}^{13}C^{18}O$	1.34(-9)	
$C^+ + {}^{13}C^{18}O \rightarrow {}^{13}C^+ + C^{18}O$	0.4(-10)	
$HCO^+ + {}^{13}CO \rightarrow H^{13}CO^+ + CO$	6.5(-10)	
$H^{13}CO^+ + CO \rightarrow HCO^+ + {}^{13}CO$	2.7(-10)	
$HCO^+ + C^{18}O \rightarrow HC^{18}O^+ + CO$	7.4(-10)	
$HC^{18}O^+ + CO \rightarrow HCO^+ + C^{18}O$	1.8(-10)	
$HCO^+ + {}^{13}C^{18}O \rightarrow H^{13}C^{18}O^+ + CO$	8.3(-10)	
$H^{13}C^{18}O^+ + CO \rightarrow HCO^+ + {}^{13}C^{18}O$	0.9(-10)	
$H^{13}CO^+ + C^{18}O \rightarrow HC^{18}O^+ + {}^{13}CO$	5.5(-10)	
$HC^{18}O^+ + {}^{13}CO \rightarrow H^{13}CO^+ + C^{18}O$	3.7(-10)	
$H^{13}CO^+ + {}^{13}C^{18}O \rightarrow H^{13}C^{18}O^+ + {}^{13}CO$	7.4(-10)	
$H^{13}C^{18}O^+ + {}^{13}CO \rightarrow H^{13}CO^+ + {}^{13}C^{18}O$	1.8(-10)	
$HC^{18}O^+ + {}^{13}C^{18}O \rightarrow H^{13}C^{18}O^+ + C^{18}O$	6.5(-10)	
$H^{13}C^{18}O^+ + C^{18}O \rightarrow HC^{18}O^+ + {}^{13}C^{18}O$	2.7(-10)	
$^{13}C^+ + CN \rightarrow C^+ + {}^{13}CN$	2.0(-10)	
$C^+ + {}^{13}CN \rightarrow {}^{13}C^+ + CN$	6.04(-12)	
$^{13}C + CN \rightarrow C + {}^{13}CN$	4.98(-10)	
$C + {}^{13}CN \rightarrow {}^{13}C + CN$	2.24(-11)	
$^{13}C + C_2 \rightarrow C^{13}C + C$	1.64(-10)	
$C + C^{13}C \rightarrow {}^{13}C + C_2$	1.22(-11)	
$^{13}C^+ + CS \rightarrow C^+ + {}^{13}CS$	2.0(-10)	
$C^+ + {}^{13}CS \rightarrow {}^{13}C^+ + CS$	9.03(-13)	

Table 2.1: Isotope fractionation reactions and their rate constants at 10 K ([19]). a(b) means a$\times 10^b$.

Species	**Abundance relative to H_2 [cm^{-3}]**
H	5(-5)
HD	3(-5)
He	9(-2)
C	1.4(-4)
^{13}C	1.9(-6)
N	7.5(-5)
O	3.2(-4)
^{18}O	6.4(-7)
F	2(-8)
Na	2(-9)
Mg	7(-9)
Si	8(-9)
S	8(-8)
Fe	3(-9)
H_2	1

Table 2.2: Initial elemental abundances used in the model ([26]). a(b) means $a \times 10^b$.

Chapter 3

Astrochemistry of HNCO isotopologues

After introducing the current knowledge of HNCO "chemistry", this section will deal with the study of the abundances of HNCO and its isotopologues, under the assumptions and the model presented above; nonthermal desorption mechanisms are, thus, not included. A short comparison with other important carbon, oxygen and hydrogen - bearing species is also presented.

3.1 Observational history

The project focuses on introducing the isotopes of the three major elements in the ISM : C, H and O. Thus, after HCO^+, isocyanic acid (HNCO) seems to be an interesting molecule since it carries all of them. HNCO is an asymmetric top molecule : the three moments of inertia are different. Consequently, the expression of its energy levels (see figure 3.1) is complicated but they are characterized by two quantum numbers : J, the total angular momentum, and K, the projection of J onto the symmetry axis of the molecule. Thereafter, levels will thus be designated as

$J_{K_{-1}K_1}$ where K_{-1} and K_1 are the projection of J onto the symmetry axis for prolate and oblate shape.

3.1.1 Tracer of dense, shocked or Far Infrared regions

3.1.1.1 Tracer of dense regions

Snyder et al. first detected isocyanic acid in 1972 towards the Sgr B2 molecular cloud, through its 4_{04} - 3_{03} rotational transition ([43]). Its emission was found to be very extended, notably near the dense core region of the molecular cloud. Subsequent studies confirm this fact : Jackson et al. found that rotational transitions such as 5_{05} - 4_{04} and 4_{04} - 3_{03} originate in high density regions ($n > 10^6$ cm^{-3}). Thus, this molecule was thought very early to trace the densest regions of molecular clouds. Since its first detection, HNCO has been observed in numerous astronomical environments with a variety of physical conditions : galaxies ([24]), hot cores ([43]), dense regions of the Galactic Centre ([24]), translucent clouds ([49]) and external galaxies ([31]).

3.1.1.2 Tracer of far infrared field

Assuming an optically thin medium and a Boltzmann distribution, Churchwell showed that the population of HNCO rotational levels could be split in two categories ([7]) :

- $E_u < 40$ K : the $K_{-1} = 0$ ladders give an excitation temperature of about 10 K and a column density of 2.4×10^{15} cm^{-2},
- $E_u > 40$ K : the $K_{-1} > 0$ ladders give an excitation temperature of about 70 K and a column density of 3.6×10^{14} cm^{-2}.

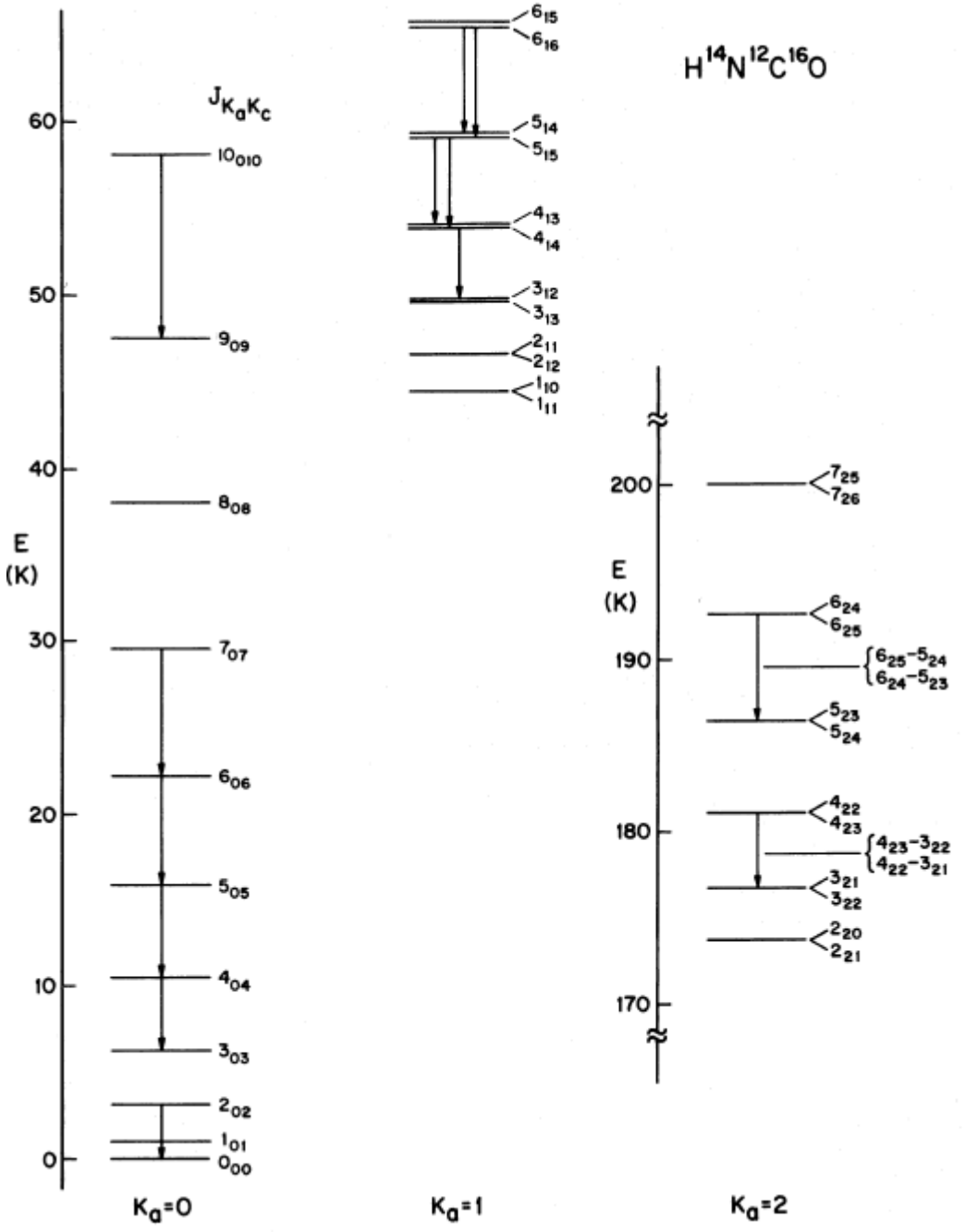

Figure 3.1: Energy levels scheme of HNCO ([7]).

However the $K_a > 0$ ladders can not be as populated by collisions as observations tend to show. Indeed, in models where collision rates are dominant, a density greater than 10^9 cm^{-3} is required, for instance, to thermalize the K_0 - K_1 transition and lead to the observational abundances. However, such a density is not reached in the core of Sgr B2, where they perform their study. Thus, Churchwell suggested that transition rates are dominated firstly by radiative processes rather than collisional ones. Consequently, HNCO (its transitions with non-zero K_{-1}) could probe the far infrared (FIR) radiation field under some conditions.

3.1.1.3 Tracer of shocked regions

In addition to being a good dense regions and FIR radiation tracer, isocyanic acid also traces shocked regions ([37]). Rodriguez et al. measured the highest abundances of HNCO relative to H_2 towards the protostar L1157 and its molecular outflow which presents signature of shocks. They also found that HNCO emission lines are similar to those of CH_3OH or SO which are well known shock tracers. In this particular case, the following pathway can explain the enhancement in HNCO gas phase abundance : dust grain mantles are processed by shock waves, ejecting a high amount of molecules in the gas phase; then neutral-neutral reactions occur in this gas phase.

Martin et al. recently conducted a survey of thirteen molecular clouds in the Galactic centre region and proposed that the abundance ratio between HNCO and CS could be a way of distinguishing between shock and radiation activity in a molecular cloud ([25]). Indeed, this ratio is highly contrasted between all sources and they managed to divide them in three groups : giant molecular clouds with the highest ratios, photodissociated regions with the lowest ones and a third group with intermediate values consisting of hot cores.

3.1.2 Formation of HNCO

Since its discovery, many assumptions have been made on how this molecule is formed. When considering dense molecular clouds, the hydrogen density lies between 10^4 and 10^6 cm^{-3}. Iglesias first suggested a gas phase chemistry for HNCO formation assuming that only high-energy cosmic rays can penetrate the cloud (UV photons and low-energy cosmic rays are expected not to). The formation pathway is through ion-molecule reactions ([14]):

$$H_2 + CNO^+ \rightarrow H + HNCO^+ \text{ with k} \approx \text{1.0E-9 cm}^3\ \text{s}^{-1}$$

$$H_2 + HNCO^+ \rightarrow H + H_2NCO^+ \text{ with k} \approx \text{1.0E-9 cm}^3\ \text{s}^{-1}$$

$$H_2NCO^+ + e^- \rightarrow H + HNCO \text{ with k} \approx \text{5.0E-7 cm}^3\ \text{s}^{-1}$$

Turner et al. later on considered also a gas phase formation, but involving different species ([49]) :

$$CN + O_2 \rightarrow NCO + O$$

$$NCO + H_2 \rightarrow HNCO + H$$

The destruction of HNCO occurs mainly when it interacts with H_3^+ and He^+ but ions such as H^+, HCO^+ or H_3O^+ can also destroy isocyanic acid.

These formation pathways are highly questioned since they fail to reproduce observed abundances, whatever physical conditions are, though they can succeed in a few environments under precise conditions. It is now known that gas phase only can not explain HNCO abundances in the gas phase of the ISM. Grain surface chemistry has an important role to play. HNCO gas phase abundance could be

explained by thermal desorption from dust grain surface ([16], [46]). Garrod et al. were the first to introduce this alternative in chemical models ([10]). HNCO is supposed to be formed on grain surfaces when radicals (generally, unsaturated molecules or molecules with unpaired electron) CO and NH react together. This Hydrogenation of accreted NCO could be represented by the following reaction :

$$\text{G-H} + \text{G-NCO} \rightarrow \text{G-HNCO}$$

where G corresponds to grain surface species.

Subsequently, isocyanic acid is desorbed into the gas phase either by thermal or non thermal mechanisms.

Table 3.1 shows some observations of HNCO in different astronomical environments.

Object	**T_{ex} [K]**	**Column density [10^{13} cm^{-2}]**	**Relative abundance [10^{-9}]**	**Reference**
Sgr B2	12.8	45 - 64		[43]
		240	2.4	[7]
Sgr B2(N)		6000	>20	[16]
Sgr B2 (HNCO(SW))	10	70		[16]
Sgr B2(M)	36	100	0.5	[16]
Orion A	25	74	8.7	[56]
Sgr A	$\approx$ 10	$\approx$ 100	$\approx$ 10	[56, 15]
Dense cores	24-236	4 - 70	0.22 - 8.7	[56]
TMC 1	>9	0.9		[15]
Seyfert galaxies (NGC 253)	20-50	1-50	1.2 (4)	[31, 15, 24]
SN remnant (W51)	>10	3		[15]
HII (ionized) region	$\approx$ 10	1.5		[15]
Galaxy (ex : IC342)	<10	2-12	0.2-0.55	[31, 24]
starburst galaxies	5	10	1-6.3	[24]
L1157-B2 (dark cloud)			25-96	[37]
Translucent clouds			0.2-5	[49]

Table 3.1: Temperature, column density and relative abundance of HNCO in different astronomical environments.

3.2 Relative abundance of HNCO

3.2.1 Gas phase formation

Using the updated chemical network, the relative (to H_2) abundance of HNCO is studied in this section. From figure 3.2, two regimes seem to exist depending on the density. For (relatively) low densities, there is a significant hollow in abundance between 10^5 and 10^6 years (red rectangle) which does not exist for higher densities. HNCO isotopologues show the same behaviour with lower abundances.

A developed short program allows us to determine which reactions contribute the most in the abundance of a particular species. It also enables us to see the ranking between all the reactions either for formation or destruction pathways and the rate contribution as a percentage of each reaction.

When the time belongs to [10^5 : 10^6 years], HNCO is mainly produced via dissociative recombinations involving $HNCOH^+$ and H_2NCO^+. Not surprisingly, for densities of typical molecular cloud, cosmic ray ionisation is important. Thus, HNCO is mainly destroyed by cosmic rays (> 99 %). For very low densities (around 10^3 cm^{-3}), H_2NCO^+ is responsible of HNCO formation by more than 97 % whereas for higher densities it is more balanced : > 50 % and > 40 % for respectively $HNCOH^+$ and H_2NCO^+. This could explain the disappearance of the hollow since these two species present the same shape as HNCO.

In addition, except at steady state in some cases, the relative abundance of HNCO seems a little underestimated in these models, comparing with table 3.1. As previously mentioned, grain surface chemistry plays an important role for isocyanic acid production. Thus, gas grain interactions are added in the model.

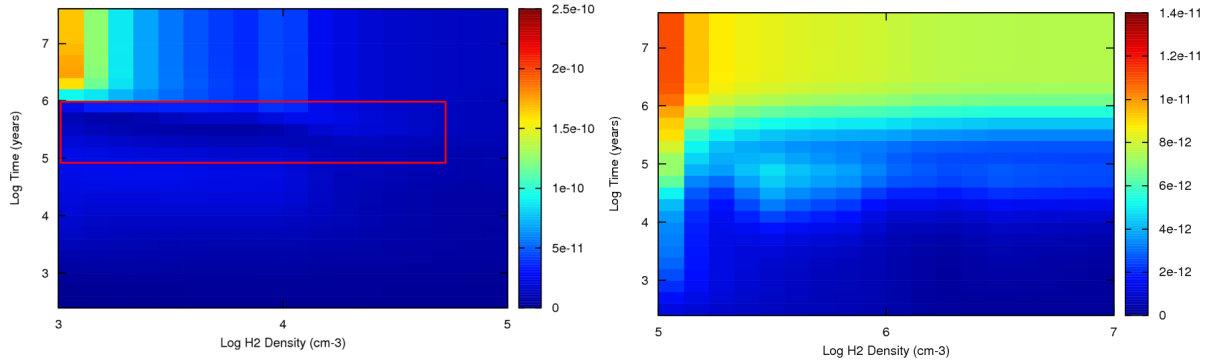

(a) Low densities. (b) High densities.

Figure 3.2: Density - time chromatic plot for the abundance of HNCO.

3.2.2 Adding gas grain interactions

Here, the abundance on grains is not followed as the freezout is allowed just by adding an extra destruction term in the differential equation of each species. This term depends on the temperature (T), the density of the cloud (n) and the mass (m) according to the following equation :

$$\frac{d\mathrm{N(X)}}{dt} = 5.2 \times 10^{-17} \times \sqrt{3.33 \times 10^{-3} \times \mathrm{T}} \times \mathrm{n} \times \frac{1}{\sqrt{\mathrm{m}}} \times \mathrm{N(X)} \qquad (3.1)$$

where N(X) is the relative abundance of species X. The square root comes from the velocity dependence. And the first constant depends on the grain number density and its cross section.

Including the possibility of accretion on grain surfaces leads to a decrease in species abundances. Carbon monoxide is one of the key species; when its abundance starts to change (see figure 3.3), then the other ones should change too. Figure 3.4 shows the influence of gas grain interactions on the abundance of HNCO for different densities. Differences arise only after the depletion of CO. Except for n = 10^5 cm^{-3}, the abundance is higher until the reservoir of CO drops in abundance. After this time, the truthfulness of the results can be questioned as the model does not allow the temperature to vary. This can lead to evaporation of ice mantles and as a

result an increase of gas-phase abundances. At densities as low as 10^3 cm^{-3}, there is almost no difference between the gas phase model and the one including grain surface chemistry. However, in other cases, differences can be significant between a few 10^4 and 10^5 years depending on the density even if they are almost non-existent for very early times.

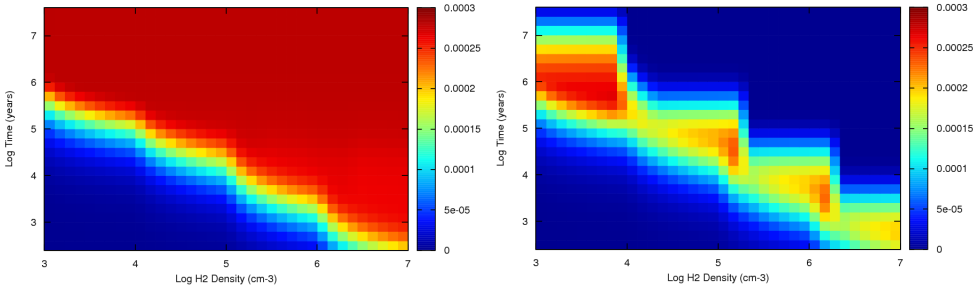

(a) Gas phase only. (b) Gas grain interactions included.

Figure 3.3: Influence of gas grain interactions on the temporal and density variations of the abundance of CO.

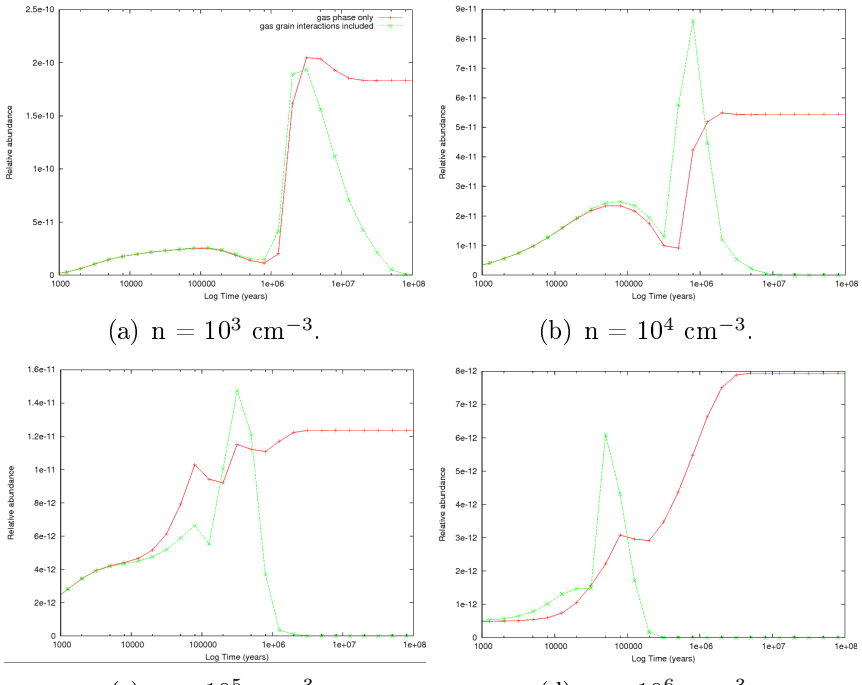

(a) n = 10^3 cm^{-3}. (b) n = 10^4 cm^{-3}.

(c) n = 10^5 cm^{-3}. (d) n = 10^6 cm^{-3}.

Figure 3.4: Influence of gas grain interactions on the temporal variations of the abundance of HNCO. The red line represents the gas phase model; the green line, the model including grain surface chemistry.

3.3 Modelling HNCO isotopologues

Density dependences are investigated for isocyanic acid and its isotopologues along with their fractionation ratios.

3.3.1 Isotope ratios as a function of density and time

To investigate the density dependence, 37 models were performed for a temperature of 10 K with densities ranging from 10^3 to 10^7 cm^{-3}. Figures 3.5, 3.6, 3.7 and 3.8 present chromatic density-time plots for HNCO isotopologic ratios. As might be expected, these isotopic ratios show variations which, depending on time and temperature considered, can be either strong or weak, except for the carbon ratio which seems more homogeneous (its variations are tiny).

3.3.1.1 Deuterated ratio

The hydrogen isotopic ratio, DNCO/HNCO, ranges from about 0.001 to 0.008. The lowest value occurs at high density between 10^4 and 10^5 years whereas the highest value occurs at steady state ($t > 10^7$ years) for a relatively low density ($n \approx 10^4$ cm^{-3}). The first immediate feature of figure 3.5 is the strong dependence on density. Whatever the age of the cloud is, the lowest ratios lie in densities superior to 10^5 cm^{-3} and the highest ones below this limit.

At high densities there is less CO, N_2, e^-, for instance, to convert H_3^+ into HCO^+, N_2H^+, H_2 but more HD to convert it into H_2D^+ which will produce more deuterated species. Thus, deuterated ratios are expected to increase with density. In the case of HNCO, this is partially right. Indeed, when the density increases from 10^3 to 10^5 cm^{-3}, the ratio increases as well. However, it starts to decrease after 10^5 cm^{-3} even more strongly than it has risen.

At density fixed, the temporal variations are not so strong. After a density of 2×10^4 cm^{-3}, the same behaviour occurs : the ratio decreases and then increases until it reaches its maximum at steady state. The minimum ratio occurs earlier for higher densities than lower densities.

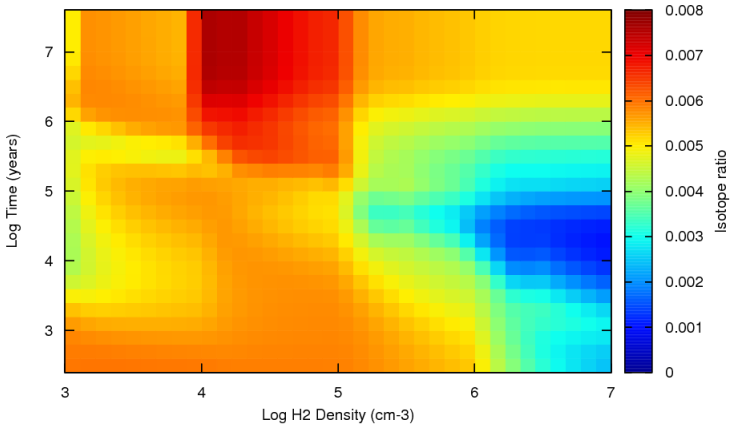

Figure 3.5: Density - time chromatic plot for the ratio DNCO/HNCO at a temperature of 10 K.

3.3.1.2 Carbon isotopic ratio

At low densities, below 10^4 cm^{-3}, the fractionation is very high around 10^6 years and reaches 450 for n = 2×10^3 cm^{-3}. Nevertheless, at higher densities, even if the fractionation is high for a narrow range of time, generally the temporal variations are tenuous, as shown by figure 3.6. The HNCO to HN^{13}CO ratio remains close to the underlying ratio (here, 75).

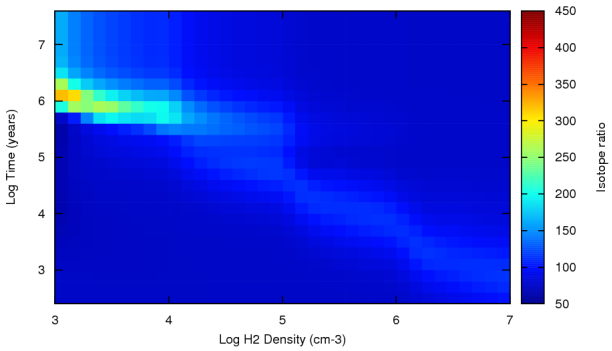

Figure 3.6: Density - time chromatic plot for the ratio HNCO/HN^{13}CO at a temperature of 10 K.

3.3.1.3 Oxygen isotopic ratio

According to figure 3.7, the ^{18}O chemistry occurs much later than the carbon and hydrogen isotopes one. Whatever the density is, the ratio between HNCO and $HNC^{18}O$ remains equal to the underlying oxygen ratio (500) until, at least, 10^5 years. Then, both density and time dependences are strong. The lowest values (about 500) occur at early times whatever the density is and the highest ones (about 830) occur at high densities ($n > 10^6$ cm^{-3}) at steady state.

After 3×10^5 cm^{-3}, the ratio keeps increasing until steady state where it has increased by more than 50%. For other densities, it reaches a maximum and decreases a little to its steady state where it is still much higher than the underlying ratio. Whatever the density is, the increase is steep.

It is also worth noting that this ratio presents two different temporal regimes :

- After 2×10^6 years, when increasing the density, the ratio first decreases and then increases. Though, these variations are not big, except for $t = 3 \times 10^6$ years.
- Between 10^5 years and 2×10^6 years, the opposite phenomena occurs : the ratio first increases with density and then decreases. Variations are stronger than in the first regime.

In addition, figure 3.8 shows that the ratio $HN^{13}CO/HNC^{18}O$, which contains two minor isotopes, undergoes slight variations around the initial value, which should be $500/75 \approx 6.67$.

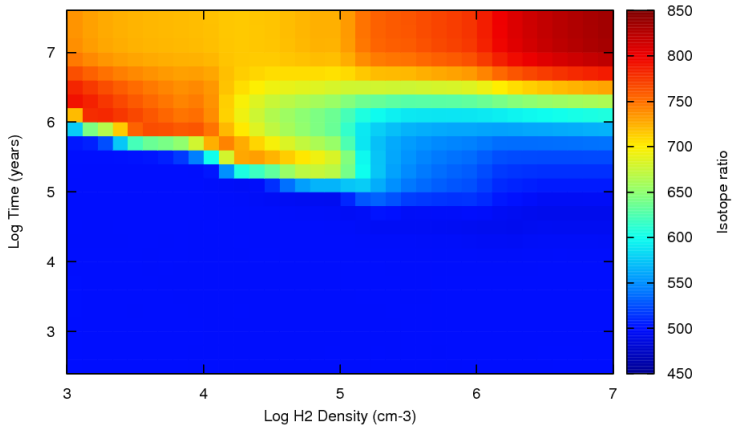

Figure 3.7: Density - time chromatic plot for the ratio HNCO/HNC^{18}O at a temperature of 10 K.

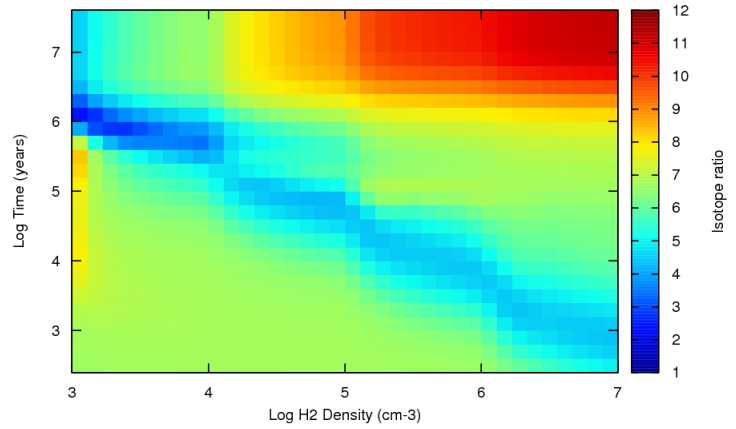

Figure 3.8: Density - time chromatic plot for the ratio HN^{13}CO/HNC^{18}O at a temperature of 10 K.

3.3.2 Comparison with CO, HCO^+ and H_2CO

Langer et al. ([19]) separated the carbon isotope ratios in three categories : CO, HCO^+ and the "carbon isotope pool". As the main elements are particularly interesting, HNCO will be compared with CO, HCO^+ and H_2CO in the following subsections.

3.3.2.1 CO isotopologues

CO exhibits simple behaviour both for carbon and oxygen fractionation. In the first case, very little fractionation occurs. The ratio CO/^{13}CO lies between 50 and

75 and the lowest values occur at low density between 10^4 and 10^5 years. Density and temporal variations are similar : after 10^3 years, the ratio increases with both, except around 10^3 cm^{-3}.

This behaviour is even stronger for oxygen fractionation. Before 10^6 years, the CO/C^{18}O remains constant at about 500, the underlying oxygen ratio, whatever the age and density are. At steady state, it reaches its maximum : about 650 at 10^3 cm^{-3} and increasing with density until about 850 at 10^7 cm^{-3}.

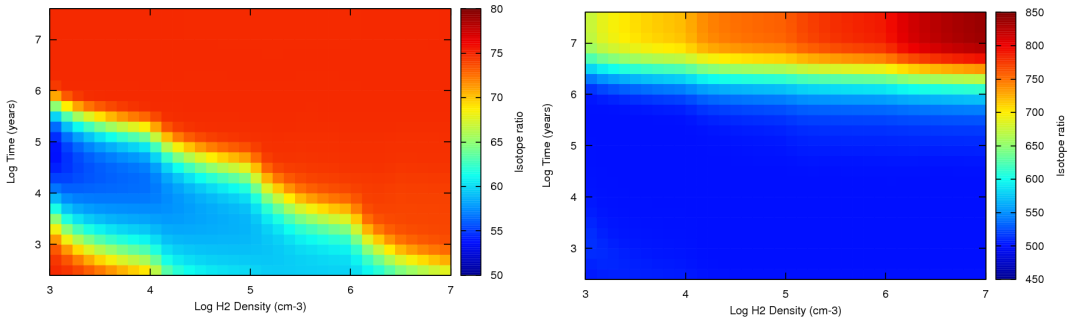

(a) ^{12}CO/^{13}CO. (b) C^{16}O/C^{18}O.

Figure 3.9: Density - time chromatic plot of CO isotopologic ratios.

3.3.2.2 HCO$^+$ isotopologues

The behaviour of HCO$^+$ isotopologues is more complex than HNCO ones. First, the DCO$^+$ to HCO$^+$ ratio extremes occur in an opposite way of those of HNCO : at very early times (t $< 10^3$ years) for the highest values whatever the density is and at steady state and low density for the lowest values. This ratio shows different regimes with density and time. On one hand, at densities lower than 10^5 cm^{-3}, this ratio decreases with time whereas after this density, the ratio first decreases and increases until steady state which is lower than early times. On the other hand, the variations with density present three regimes. Before 10^3 years, the ratio decreases with time whereas after 2×10^5 years it increases. Between, the behaviour is intermediate : it drops to reach a minimum around 10^4 - 10^5 cm^{-3} and rises again.

DCO$^+$ is quite different from other deuterated species, as stated in previous

chapter. Due to its abundance correlation with CO depletion and deuterium capability, it should be found everywhere in a dark cloud. However, it is not the case; Pagani et al suggested that the absence of DCO^+ could be the result of a high H_2 ortho-para ratio (OPR). Indeed, in their study, they showed that the detectability of this particular species enable us to constrain the OPR which leads to an upper limit on the age of the cloud. With the same parameters for a typical dark cloud as in this thesis, they found : (i) for OPR < 0.1, DCO^+ is detectable in less than 3×10^5 years; (ii) for OPR $= 0.1$, DCO^+ should be detectable around 5×10^5 years and after 2×10^6 years; (iii) for OPR > 0.1, it takes at least 3×10^6 years to observe DCO^+. Results presented in figure 3.10 for n $= 10^4$ cm^{-3}, seem to be consistent with the conclusion (ii), as the deuterated ratio drops in between these two time limits. For high densities the ratio reaches a maximum not before few mega-years. Consequently, considering the results of Pagani et al on DCO^+ and the deuterated ratio of figure 3.10, a dark cloud must be younger than few mega-years (see section 5.2).

For the HCO^+ to $H^{13}CO^+$ ratio, the behaviour is quite similar to HNCO. The variations are not strong around the underlying carbon ratio, except for densities lower than few 10^3 cm^{-3} where the ratio is doubled between 10^4 and 10^5 years.

As for the oxygen isotopic ratio, the first feature to note is that the values are always under the underlying oxygen ratio, opposite behaviour from HNCO. Apart from very few occasions, the HCO^+ to $HC^{18}O^+$ ratio decreases with density whatever the age of the cloud is. At density fixed, it starts decreasing and increases again after about 10^6 years.

3.3.2.3 H_2CO isotopologues

Figure 3.11 shows the behaviour of H_2CO isotopologues. Concerning the deuterium ratio, the difference from HNCO one is an order of magnitude but the extent of the

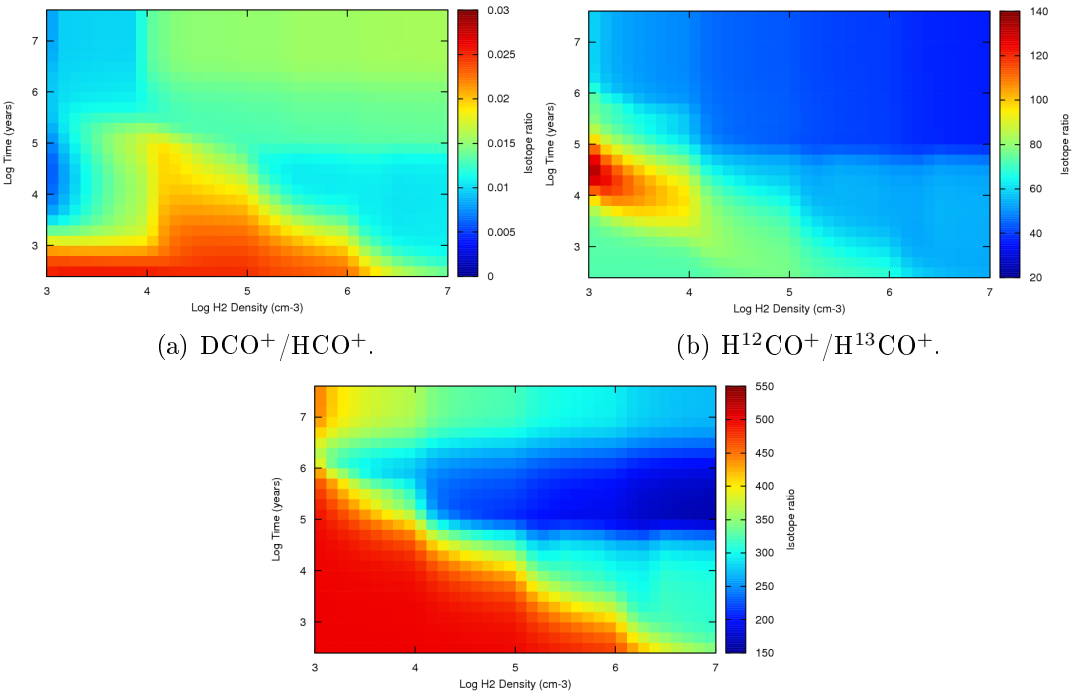

(a) DCO^+/HCO^+. (b) $H^{12}CO^+/H^{13}CO^+$.

(c) $HC^{16}O^+/HC^{18}O^+$.

Figure 3.10: Density - time chromatic plot of HCO^+ isotopologic ratios.

fractionation is similar (the highest values are about seven times the lowest ones). The general trend for $HDCO/H_2CO$ is an increase with density. The temporal variations are not as strong as the density ones but the behaviour is more complex. For densities lower than 10^3 cm^{-3}, the ratio increases simply with time. However for higher densities, an initial increase is followed by a decrease between 10^5 and 10^6 years and an increase again until steady state.

The carbon fractionation is similar to the HNCO one in the sense that the plot is really homogeneous, except at low densities around 10^6 years where the fractionation is high (five times the initial carbon ratio). Otherwise before few 10^5 years, $H_2CO/H_2^{13}CO$ remains equal to 75 and after the fractionation is bigger than for HNCO but homogeneous along time and density (around 200).

For oxygen fractionation, the behaviour is that of CO when replacing the increase by a decrease with time.

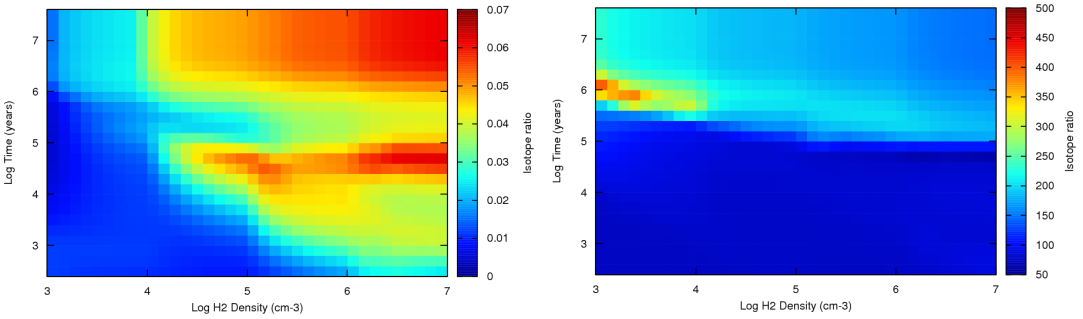

(a) $HDCO/H_2CO$. (b) $H_2{}^{12}CO/H_2{}^{13}CO$.

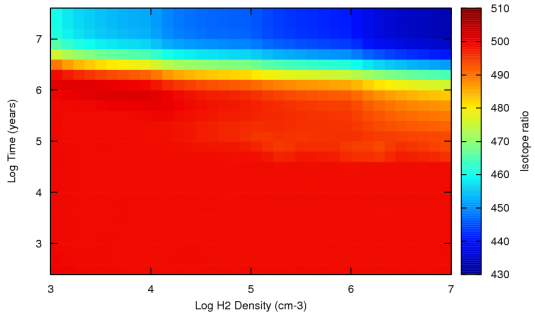

(c) $H_2C^{16}O/H_2C^{18}O$.

Figure 3.11: Density - time chromatic plot of H_2CO isotopologic ratios.

Chapter 4

Chemical tools to study a molecular cloud

In the following section, the model developed previously is used to determine chemical tools that could enable observers to assess the age of a molecular cloud and the carbon underlying ratio in that kind of environments. The model only includes gas-phase chemistry and does not account for gas-grain interactions and chemical processes occurring on dust-grains.

4.1 Introduction

4.1.1 History of some chemical clocks

Among other astrophysical issues, molecular clouds are still not completely understood. Except dynamical and chemical models, there is no consensus on what kind of observations will help to get a deeper comprehension of mechanisms occurring in such clouds, like free-collapse and star formation. One of the first key points could be the assessment of the age of the cloud. The ideal case would be to find some

species whose abundance (or abundance ratios between species) shows strong temporal variations. Then, comparisons between observations and models might give clues to the age of astronomical objects.

Stahler was the first to propose, as a chemical clock, the cyanopolyynes ($HC_{2k+1}N$, k=0, 1, 2, ...) which are observed at radio frequencies in many molecular clouds ([44]). If one assume a sequential formation (the abundance of chain k depends on that of chain k-1, see figure 4.1) and steady state abundances for the observed chains, the age of the cloud can be deduced from the necessary time to grow the longest chain. As the destruction process of cyanopolyynes on grains is most likely known, the destruction timescale is used rather than the creation one. By this procedure, the author determined that the Taurus Molecular Cloud TMC-1 should be 9.7×10^5 years old, which is greater than the free-fall collapse time.

Concerning the specific molecular cloud, Bok globule CB238, Scappini et al. ([40]) used the abundance ratios $N(NH_3)/N(CS)$, $N(NH_3)/N(SO)$ and $N(SO)/N(CS)$ to constrain its density ($\approx 10^5$ cm^{-3}) and age (about 0.5 Myr).

Not so many assumptions have been made for molecular cloud chemical clocks, mostly because of their variety, whereas for hot cores and pre/protostellar cores, more studies were performed. They all emphasize the important role of sulphur-bearing species. Charnley ([6]) and Hatchell et al. ([12]) assumed that the sulphur reservoir is H_2S, embedded in grains, which evaporates when the temperature increases during star formation. Thus, when released into the gas phase, more SO and SO_2 are subsequently produced, making ratios between these species a good function of time. However, Buckle and Fuller ([3]) noted that the accurate estimation of the age of cores requires a better knowledge of physical conditions (density, temperature and cosmic ray ionisation). Wakelam et al. ([50]) added the strong dependence of these ratios on the grain mantle composition and the atomic oxygen abundance as other difficulties to use these sulphur-bearing species as chemical clocks.

In addition, few studies were performed to find chemical clocks for Infrared Dark Clouds clumps, regions thought to be the earliest stage of massive star formation. Sanhueza et al. ([39]), based on the evolutionary sequence of Chambers et al. ([5]), showed that the ratios N_2H^+/HCO^+ and N_2H^+/HNC (see figure 4.2) increase with evolution stages, acting as chemical clocks for these cold, dense and massive environments.

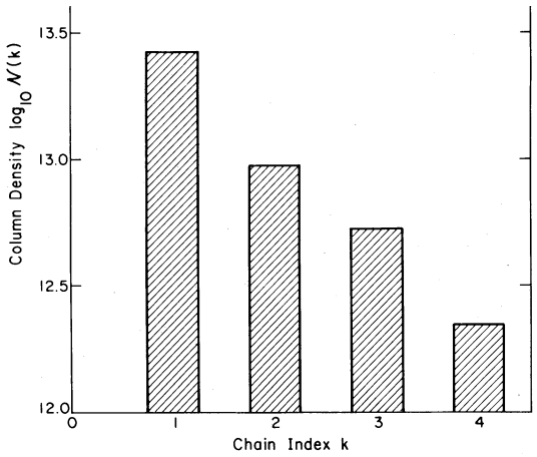

Figure 4.1: Abundance of the cyanopolyynes in TMC-1, at the NH_3 peak. The decline tends to prove the sequential formation of these molecules ([44]).

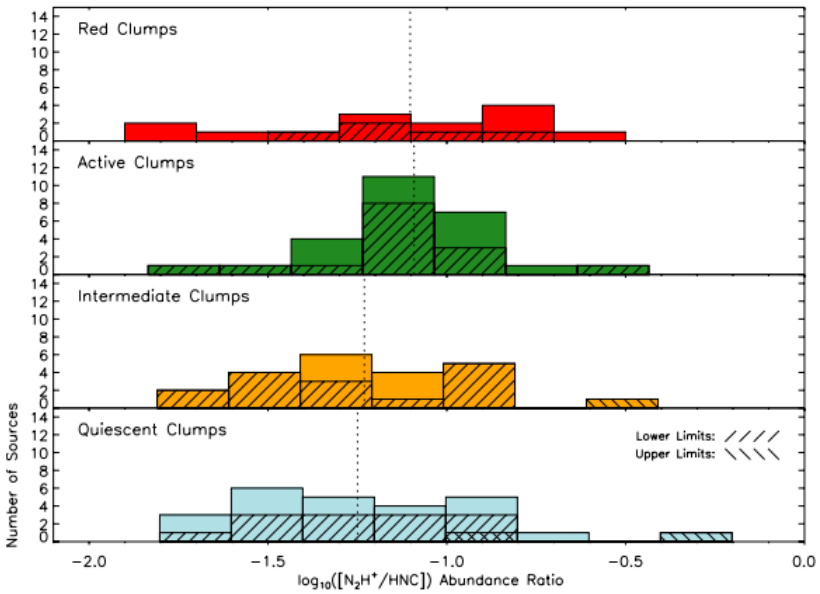

Figure 4.2: N_2H^+/HNC abundance ratio as a function of evolution stages. The vertical dashed line represent the median value for each distribution ([39]).

4.1.2 The carbon underlying ratio

The ^{13}C to ^{12}C ratio is an important parameter since it reflects the history of nucleosynthesis and chemical evolution of the Galaxy. Wilson in his review ([53]) summarized results for carbon isotopes of different studies. The important feature is the existence of a Galactic gradient in the carbon isotopic ratio. The increase in $^{12}C/^{13}C$ with distance from the Galactic Centre could be explained by the decrease in star formation activity and nucleosynthesis along this distance, which thus generate less ^{13}C. From CO and H_2CO data, he determined an interstellar isotopic ratio of 69±6 which is much higher than in the Galactic Centre ($\approx$ 20) but less than in the Solar System (89). Other studies, considering an average on numerous line of sights in many molecular clouds (CN, CH^+, CO ...) along the Galaxy, found similar $^{12}C/^{13}C$ ratios : 68±15 ([28]), 70±7 ([41]).

To measure this underlying ratio, one can use isotopologic ratios from carbon-bearing molecules but carefulness has to be paid concerning the variation around the local interstellar value, resulting from chemical fractionation (see section 1.4.2). Ritchey et al. reported observations of CN and CH^+ along with their carbon isotopologues ([35]). They claimed that $CH^+/^{13}CH^+$ and $CN/^{13}CN$ are good measure of the ambient carbon underlying ratio even if the latter undergoes fractionation.

4.2 Chemical clocks for clouds

If one wants to determine the carbon underlying ratio, an interesting feature might be the knowledge of the age of the observed cloud. It is the first step to constrain this ratio, even if no certainty can be reached. Inspired by section 4.1.1, the study focuses on some molecules related to cyanopolyynes, simple sulphur and nitrogen-bearing species. As the dependence on density and time have been investigated, it would be interesting to find a tool which exhibits similar shape for all densities and strong

temporal variations to deduce the best chemical tool for as much environments as possible.

4.2.1 "Bad" scenarios

If one could observe well the CH_3 and OH lines, which is far from being easy, the ratio between this two species abundances would be a typical "bad scenario" to use as a chemical clock. Indeed, firstly, this abundance ratio presents two different regimes according to the density as shown by figure 4.3. At very low densities (below 10^4 cm^{-3}), it increases whereas for higher densities, there is a bump around 10^4 years. In the first regime, until few 10^5 years, the ratio sticks to about 0.01 - 0.02. Then, suddenly, it is much lower around 10^{-4}. For the second regime, apart from the relatively high values (above 0.03) between few 10^3 and 10^4 years, the ratio is as low as for the steady state in the first regime. Secondly, these variations are not strong : mainly, as just mentioned, the ratio remains almost constant for large range of ages. When it changes, the difference is so sudden that it could be difficult to use it as a probe to assess a precise age. However, it could be used to say whether a molecular cloud is a young or old environment. Moreover, provided (i) the knowledge of the density and the temperature and (ii) a high signal to noise ratio, this ratio could be interesting only if observations lie in a non-constant zone. In conclusion, it is really difficult to deduce the ratio CH_3/OH observationnally and it will not be as useful as expected for our purpose.
The same scenario, with a different shape according to density, occurs with the N_2H^+/HCO^+ ratio (see figure 4.4).

In addition of this density dependence issue, another scenario is a constant increase or decrease of the chemical clock considered but with very low values and variations. The ratio between HCO^+ and HCN is a good example. Figure 4.5 shows a chromatic plot of its time and density dependences. Obviously, this ratio presents

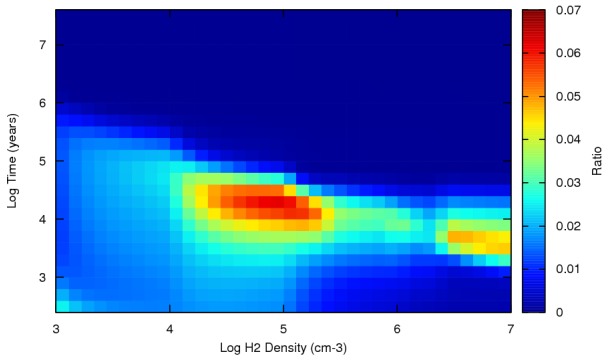

Figure 4.3: Density - time chromatic plot for the CH_3/OH ratio.

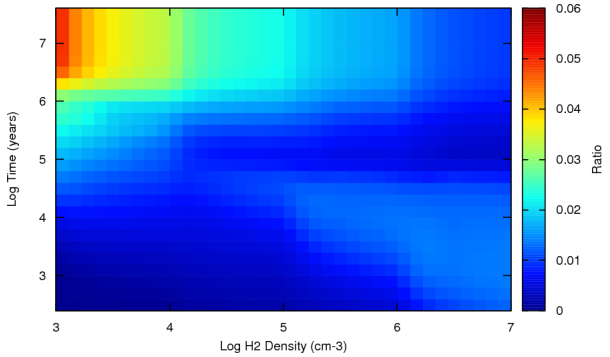

Figure 4.4: Density - time chromatic plot for the N_2H+/HCO^+ ratio.

a notable increase at low densities and late ages. Apart from this feature, it is extremely low whatever the parameters : despite few temporal variations, these low values can not be properly used to determine with enough precision the age of an environment.

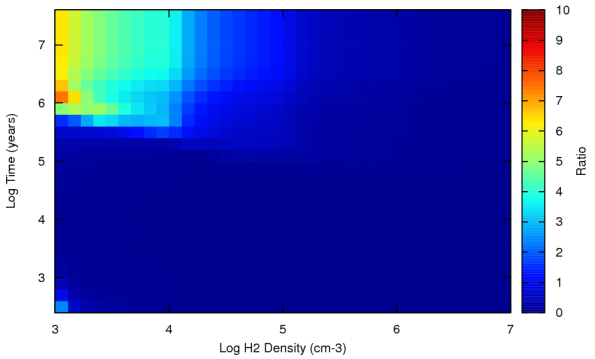

Figure 4.5: Density - time chromatic plot for the HCO^+/HCN ratio.

Finally, there is the specific case of the SO/SO_2 ratio, mentioned in Wakelam and al. paper ([50]). This ratio undergoes very large temporal variations. However,

the dependence on density is so strong that generalisation can not be done : first, the density of the environment must be determined and the question as to whether this ratio could be useful must be answered separately for each case. As shown by figure 4.6, there is at least two orders of magnitude (this increases with density) between early times and steady state. Thus, SO/SO_2 could be used to say whether a molecular cloud is young or old, more accurately than CH_3/OH. In addition, in a certain period of time where the steep decrease occurs, it could be used to assess precisely the age if the cloud lies in this range of ages.

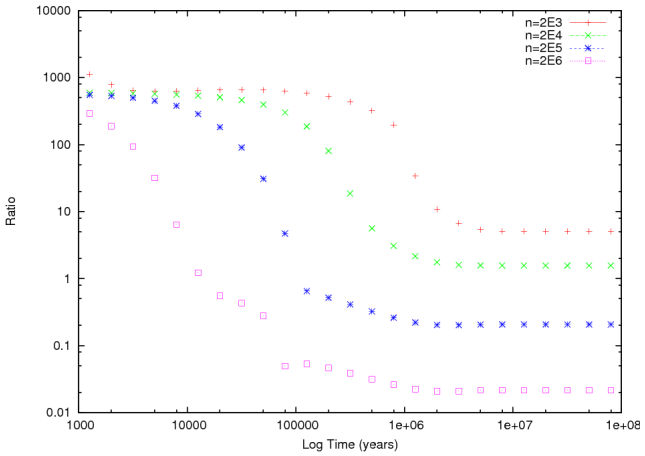

Figure 4.6: Temporal variations of SO/SO_2 for selected densities.

4.2.2 "Good" scenarios

4.2.2.1 Early times

Figure 4.7 shows a density-time chromatic plot of the ratio CS/SO. The first striking feature is that this ratio lies in a very wide range, from about 0.005 to 7500. These strong density and temporal variations are an important key to assign precisely the age of the cloud. Indeed, assuming the approximate knowledge of the density of the cloud, after a certain time, the decrease amplitude in this ratio is very large and spread over time. So, if sufficient resolution and efficiency are reached in observations, the comparison with models can help in determining the age. The

temporal variation trend is a first increase until it reaches a maximum and then a strong decrease to establish its steady state after few 10^5 - 10^6 years. Thus, for this possible clock, one also needs to assume that the age of the cloud lies in a certain range or, at least, one needs a lower limit to distinguish between the same value in the increase regime and the decrease one. The best case would be to know that the cloud is older that the time corresponding to the maximum ratio. Indeed, if one observes a ratio which can correspond to two different times in the plot : t_1, in the "increase part" before the maximum ratio R_M is reached at t_M and t_2, after t_M, in the "decrease part"; then, assuming the observer knows the cloud is older than t_M, the age of the cloud should be t_2. Moreover, the higher the density is, the higher the maximum ratio is and the earlier it occurs. For low densities ($n < 10^5$ cm^{-3}), the determination of the age is possible between few-10^4 and 10^5 years. For intermediate densities (10^5 cm^{-3} $< n <$ 10^6 cm^{-3}), it is possible between few-10^3 and just before 10^5 years. Finally for high densities, it is possible between few-10^2 and few-10^4 years. These values are representative of our model (the order of magnitude is right) but they could depend on the density since every thing is moved towards later ages while density increases.

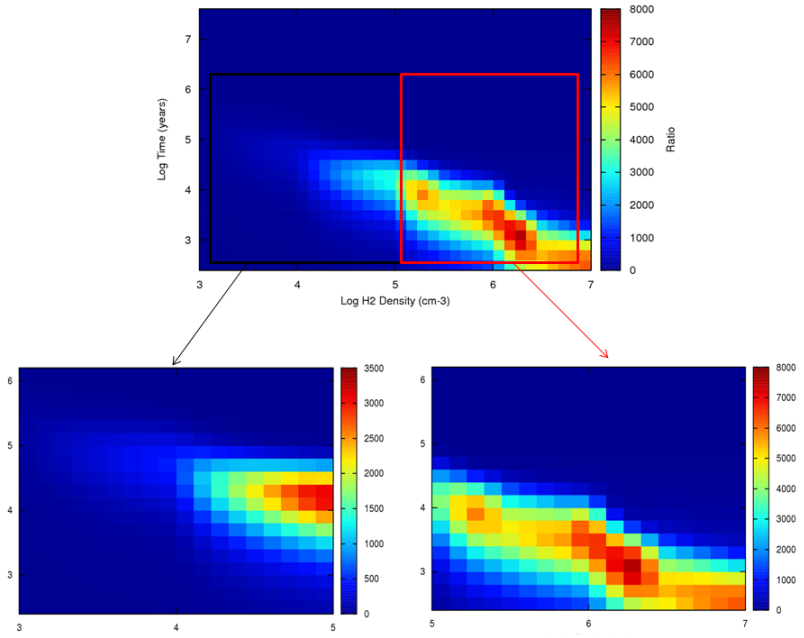

Figure 4.7: Density - time chromatic plots for the CS/SO ratio.

As indicated by other studies the ratio CS over SO could thus be used as a chemical clock. However, it is worth noting that the one between NH_3 and SO could also be useful for the same ages. Figure 4.8 shows a density-time chromatic plot of this ratio. The temporal variations are not as strong as for CS/SO but still big enough to allow precise measurements. For low densities, results are the same whereas for higher densities there are small differences. For intermediate densities, the age could be determined between 10^4 and 10^5 years. For high densities, it is possible between few-10^3 and few-10^4 years.

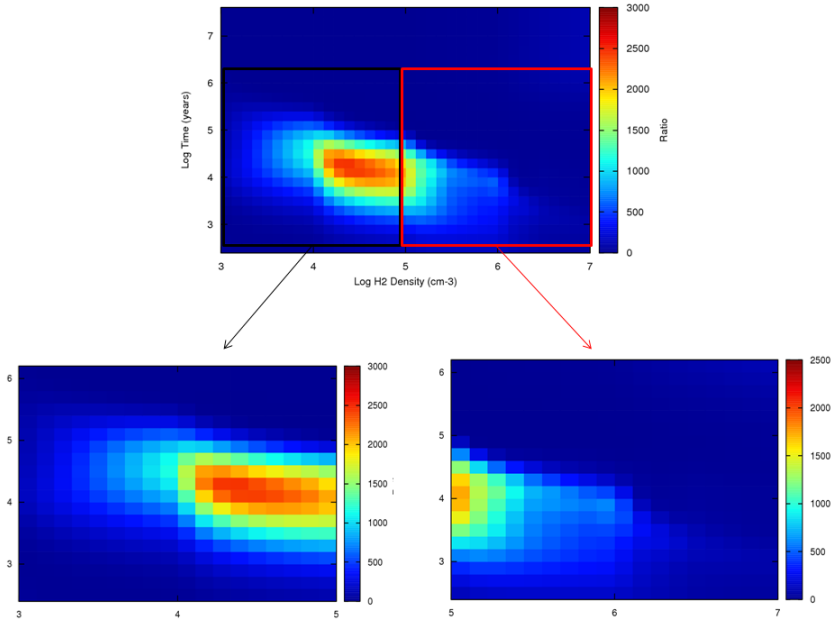

Figure 4.8: Density - Time chromatic plots for the NH_3/SO ratio.

4.2.2.2 Late ages

These previous ratios do not show strong variations after few 10^5 years. Investigations made for this project were not able to find a key ratio that works for every density and every timescale. So along with these results, few other ratios were found to have interesting features.

Figure 4.9 shows a density-time chromatic plot of the ratio NH_3/HCN. The temporal variations are much less extended than for CS over SO, but the range

is still wide enough : generally, from about 0.1 to 145 (more than three orders of magnitude). For very high density, the contrast is even bigger : the ratio is lower than 10^{-3} at early times and keeps increasing until it reaches steady state at about 140. This ratio has the simple particularity of just increasing with time, whatever the density is, until steady state. The higher the density is, the higher the maximum ratio is. Consequently, determining the age of a cloud could be easier than in the previous section : no assumptions are needed since no confusions can be made when comparing models and observations. However, the variations are only strong and steep after 10^5 years. Then, steady state is reached around 10^7 years. Thus, it is a tool for quite evolved clouds only. A very similar ratio is the one between NH_3 and HNC which is plotted in figure A.1 in appendix A.

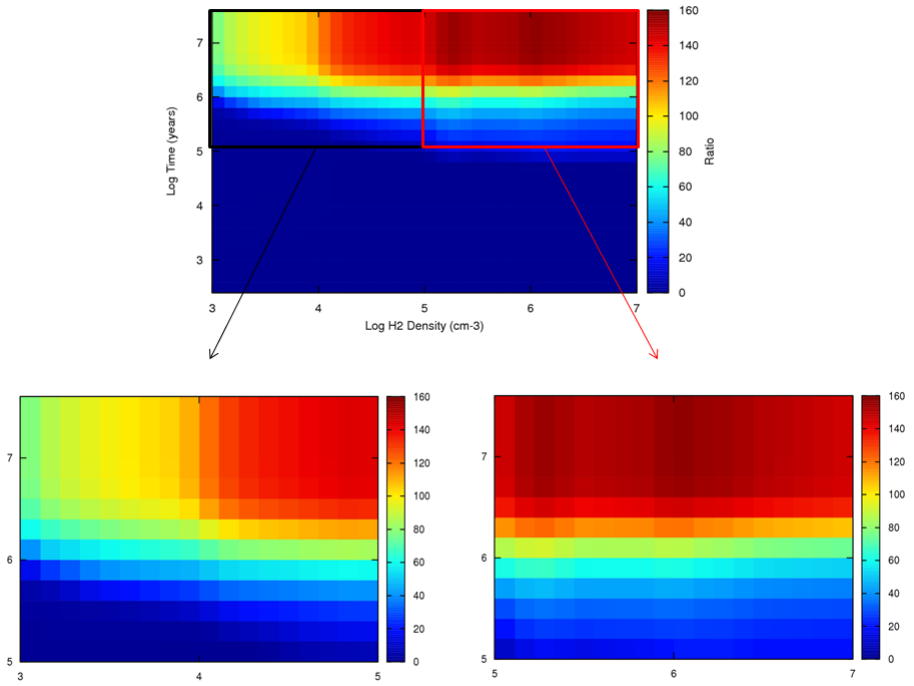

Figure 4.9: Density - time chromatic plots for the NH_3/HCN ratio.

The ratio between NH_3 and HCO^+ is also interesting for several reasons. First, because the variations are stronger for densities superior to 10^4 cm^{-3} : the ratio lies in the range [2:1870]. Second, because it could also be used for younger clouds, with the condition that its density is high ($n > 10^6$ cm^{-3}).

Finally, the ratio between N_2H^+ and HCN exhibits the same increase after 10^5 years (see figure A.2 in appendix A) and could be seen as a possible chemical clock for old objects. However, the values are quite low and should be treated with extreme caution if one wants to assess the age of an object.

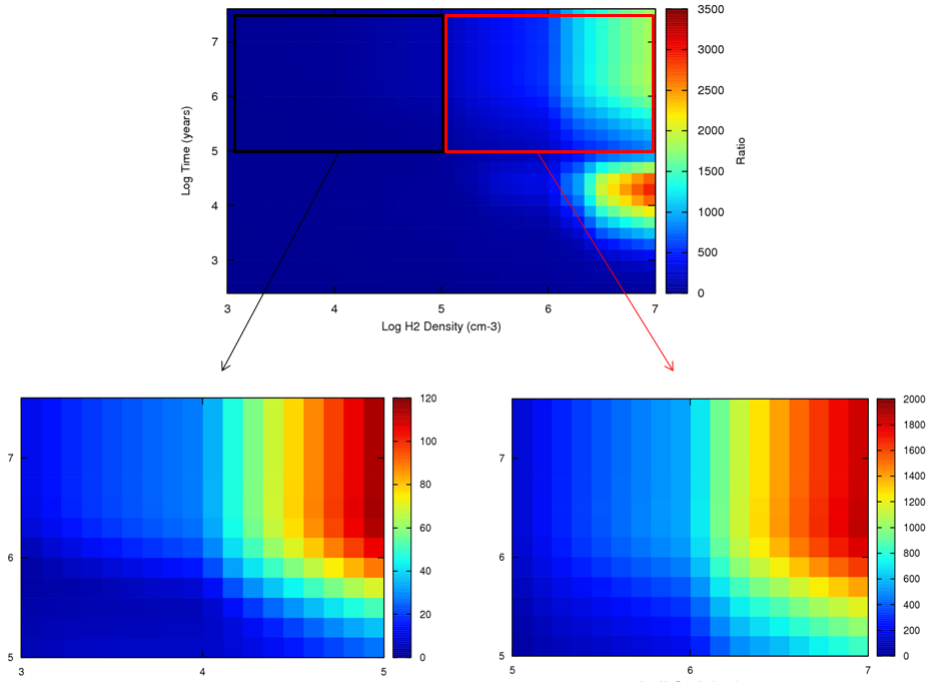

Figure 4.10: Density - time chromatic plots for the NH_3/HCO^+ ratio.

4.3 Determination of the carbon underlying ratio

Once the age of the cloud is determined with more or less precision, it is possible to work out the carbon underlying ratio. First for the typical value of 75 for the carbon underlying ratio, models were performed for densities ranging from 10^3 to 10^7 cm^{-3}. To distinguish between different possibilities, one needs to find an abundance or a ratio whose temporal variations have a particular shape. The ideal case would be the following. The chosen parameter (abundance or ratio) must be constant over the period of time, Δt, considered to be the age of the cloud (the previous tools allow us to know that). In addition, the same shape must occur for different underlying

carbon ratios and the curves corresponding to these ratios must be quasi parallel so that no confusion can be made to determine the right one : if in Δt, an intersection exists between curves, no conclusion can be made.

For instance, the carbon isotope ratios of CH_3 (see figure 4.11) and CN (see figure 4.12) are not considered as good probes. In general, they have too large temporal (and density) variations. Consequently, the carbon underlying ratio can not be assessed properly since the same abundance ratio (either $CN/^{13}CN$ or $CH_3/^{13}CH_3$) will occur for different values of the underlying ratio in a narrow range of ages. A high precision in the determination of the age of the molecular cloud is to be reached to use that kind of ratio. However, they match the previous scheme and thus could be interesting for some rare exceptions : at very low densities, below 10^4 cm^{-3}, for $CN/^{13}CN$ and around few 10^4 cm^{-3} for $CH_3/^{13}CH_3$.

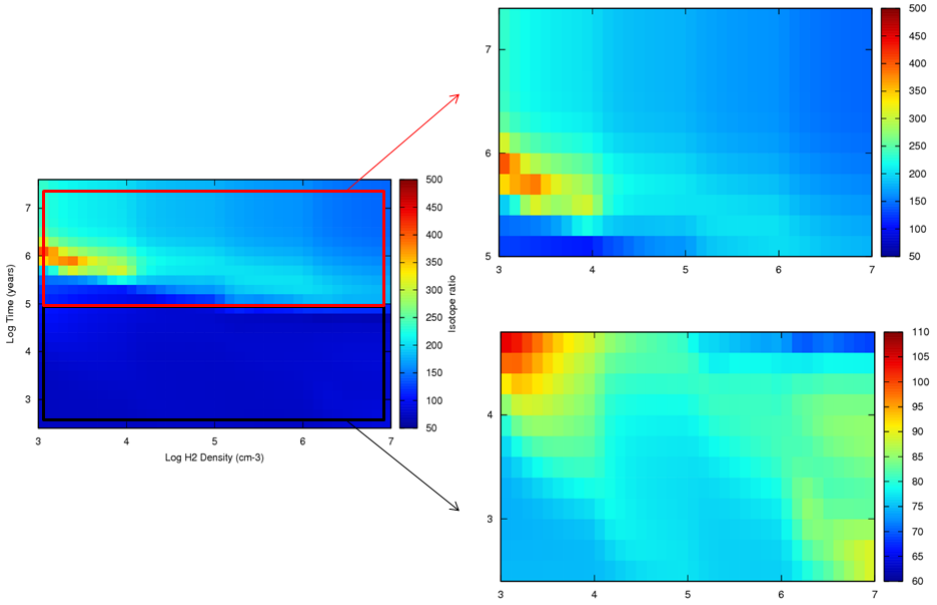

Figure 4.11: Density - time chromatic plots for the $CH_3/^{13}CH_3$ ratio.

Provided these features, comparing models and observations allow us to determine the expected $^{12}C/^{13}C$. This ideal case would probably be the ratio $^{12}CO/^{13}CO$. However, the carbon monoxide is optically thick which makes the measurements harder. Thus, other ratios or abundances need to be investigated to facilitate the

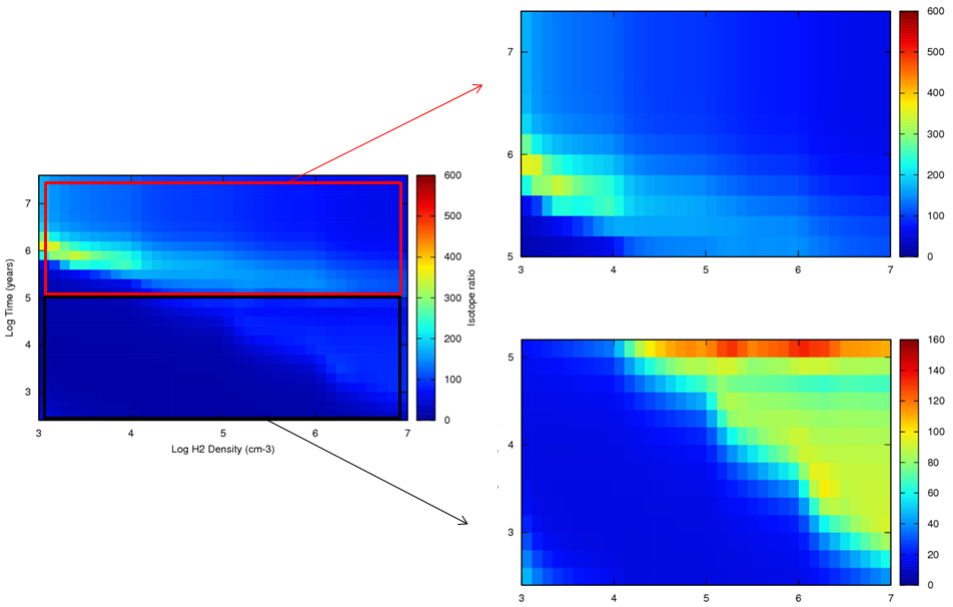

Figure 4.12: Density - time chromatic plots for the CN/^{13}CN ratio.

observations. In this work, a universal tool has not been found but, as for the previous section, different ratios appear interesting for early times and later ages.

4.3.1 Early times

Figure 4.13 shows the temporal and density variations of the HNC carbon isotope ratio, for $^{12}C/^{13}C = 75$. Until around 10^5 years and after 10^6 years, depending on density, the ratio HNC/HN^{13}C remains almost constant (except at high densities where the temporal variations become significant). For a particular density, several models were performed with different underlying carbon ratios. As expected, the difference observed between these models is only a translation. For instance, the carbon isotopic ratios (HNC/HN^{13}C in this section) are separated by a factor 75/60 between the models corresponding to these carbon ratios. Consequently, the appearance of the chromatic plots does not change : only the values of the ratio does. Figure 4.14 represents the time dependence of the ratio HNC/HN^{13}C, against the carbon underlying ratio value at n = 2×10^4 cm^{-3}.

HNC/HN^{13}C could thus be used to assign the underlying carbon ratio for clouds younger than 10^5 years and older than few - 10^6 years. However, for older clouds, another ratio seems to be better.

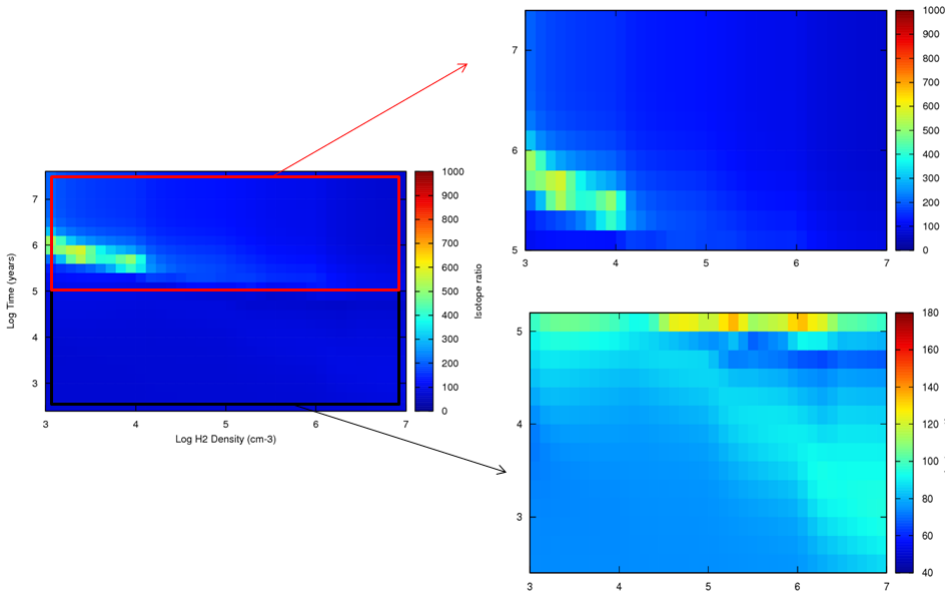

Figure 4.13: Density - time chromatic plots of the ratio HNC/HN^{13}C.

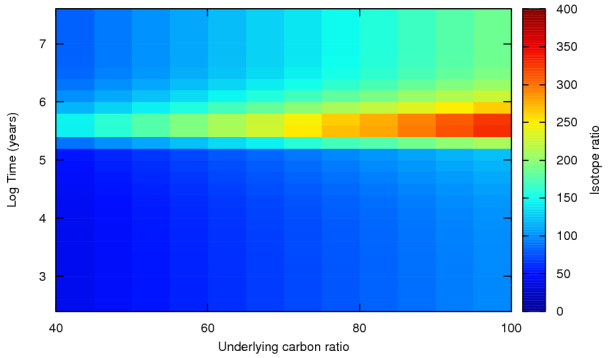

Figure 4.14: ^{12}C/^{13}C - time chromatic plot of the ratio HNC/HN^{13}C at n = 2×10^4 cm^{-3}.

4.3.2 Late ages

Figure 3.10 shows the temporal and density variations of the HCO$^+$ carbon isotope ratio, for ^{12}C/^{13}C = 75. After 10^5 years, the ratio HCO$^+$/H^{13}CO$^+$ remains constant, except for low densities. Thus, it could be used to assign the underlying carbon

ratio for clouds older than 10^5 years (see figure 4.15), which is complementary to the previous result.

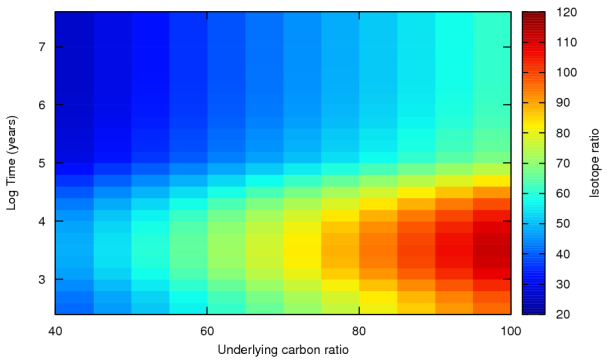

Figure 4.15: $^{12}C/^{13}C$ - Time chromatic plot of the ratio $HCO^+/H^{13}CO^+$ at n = 2×10^4 cm^{-3}.

Another ratio is found to possibly probe the carbon underlying ratio for old molecular clouds : the one between CH^+ and $^{13}CH^+$. Indeed, figure 4.16 shows the temporal variation of this ratio and despite some fluctuation, it seems to remain around 110 after few 10^5 years for all densities above few 10^3 cm^{-3}. The same conclusion arises for younger clouds but with relatively low densities. Figure 4.17 shows the dependence of this ratio on the value of the carbon underlying ratio for a density of 2×10^4 cm^{-3}. $CH^+/^{13}CH^+$ is not as perfect as the ratios previously mentioned but could be seen as an alternative to assess the carbon underlying ratio, though the precision will be less than with the others reported in this work. It should be mentioned that CH^+ is difficult to observe, notably its ground-state rotational transition which lies in the submillimetre range and near an atmospheric line of water vapor. However, this ion and its isotopologue have now been detected with Herschel both in emission and absorption towards massive star forming regions ([8]) and the ratio $CH^+/^{13}CH^+$ determined ([8], [4], [35]).

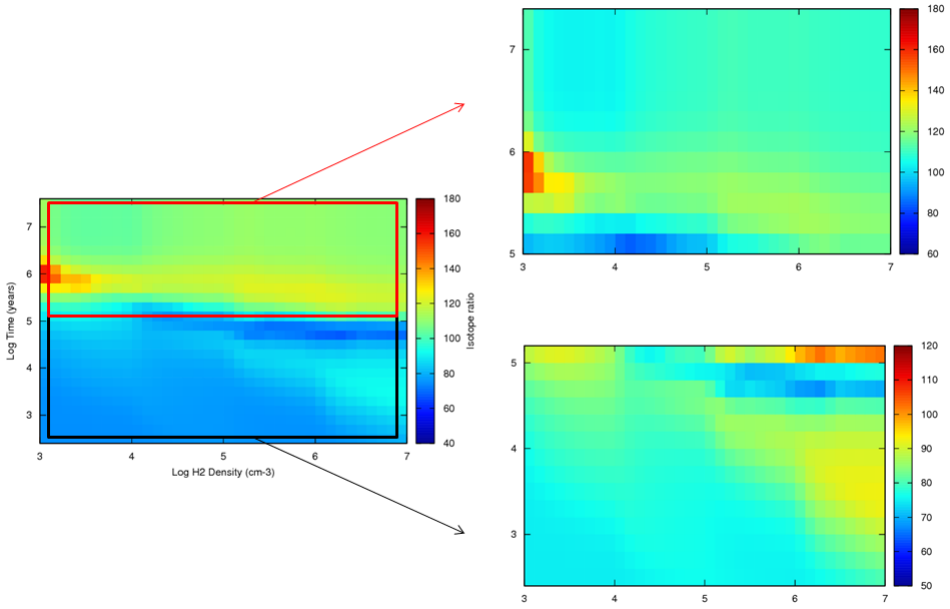

Figure 4.16: Density - time chromatic plots of the ratio $CH^+/^{13}CH^+$.

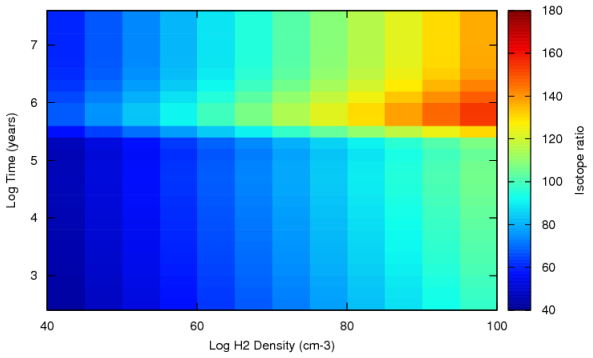

Figure 4.17: $^{12}C/^{13}C$ - time chromatic plot of the ratio $CH^+/^{13}CH^+$ at n = 2×10^4 cm^{-3}.

4.4 Summary

Figure 4.18 sums up the good chemical tools studied in this thesis along with the range of densities and/or time where they can be used to help understand a molecular cloud. When no range of densities or time are mentioned, the tool can be used for all densities and for either early or late ages. When a range of densities is associated with a range of time, it means that for these particular densities the tool only applies for these times.

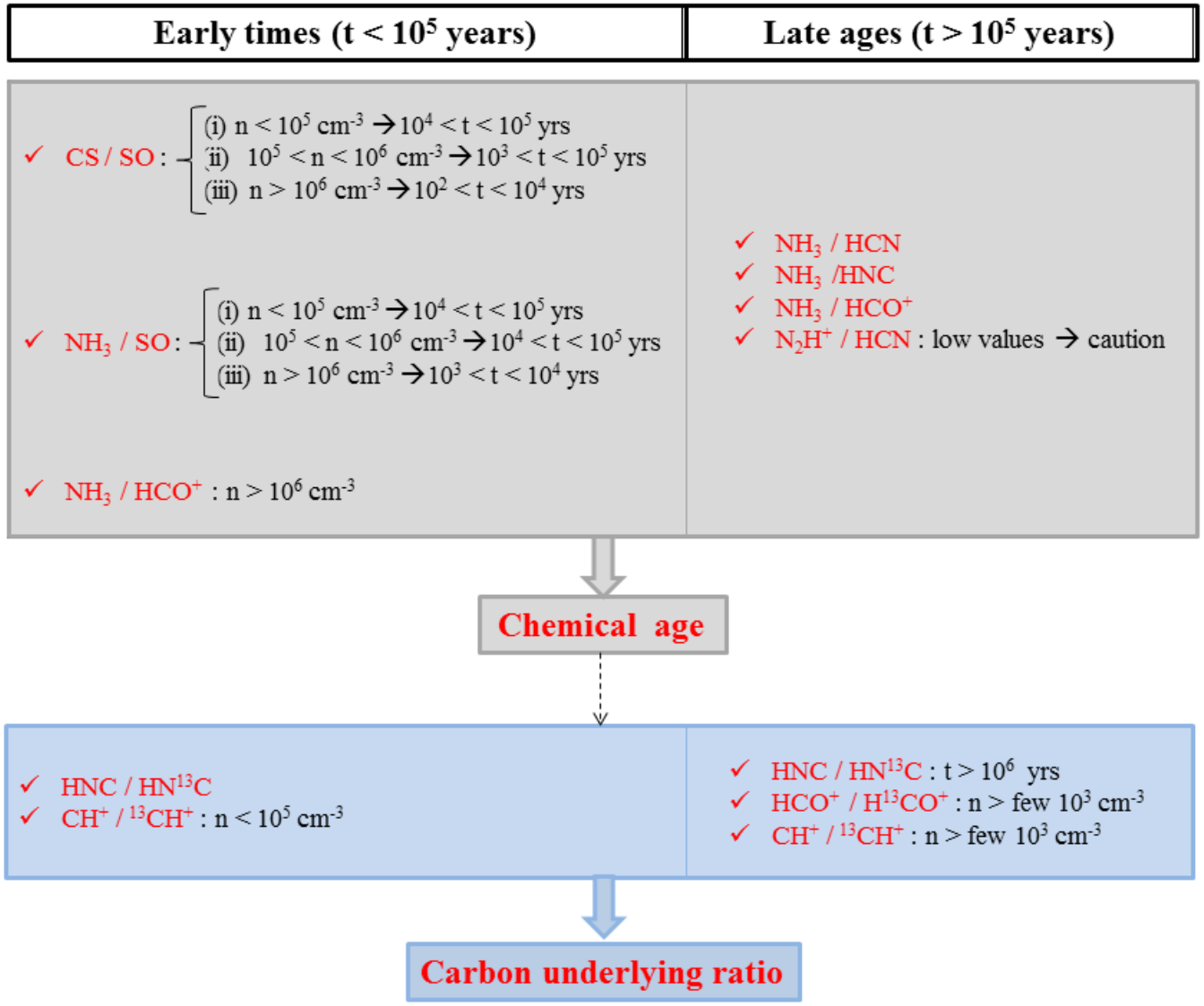

Figure 4.18: Scheme of the chemical tools useful for the determination of the chemical age (grey box) and the carbon underlying ratio (blue box) in a molecular cloud, either for early times or late ages.

Chapter 5

The Taurus Molecular Cloud TMC-1

To extend our results to many species, it is important to compare the model with observations for fundamental molecules. In order to do this, the source has to be well known in a chemical point of view : qualitatively and quantitatively, abundance measurements for many species should be available.

5.1 Presentation

The Taurus Molecular Cloud (TMC), lying in the Taurus constellation, is one of the nearest (140 pc away from the Earth) large star formation region. TMC-1 is a dark ($A_v > 2.4$ mag) and cold (T $\approx$ 10K) cloud ([9]). For decades it has been the testbed for studies on interstellar chemistry and theories on low-mass star formation. Though, no consensus has been found to explain its very rich and diversified chemistry. Indeed, TMC-1 presents a wide variety of chemistry species from cyanopolyyne (CP) group to species produced by H_3^+ (NH_3, HCO^+ ...) (figure 5.1), along with their isotopologues. For instance, this cloud presents an enhancement in deuterated species; many of them have been observed at the CP-peak to work out their D to H ratio. This peak is the southeastern region of TMC-1 ridge where carbon-chain

species exhibit their greatest emission. Thus, to test the model, TMC-1 observations at the CP-peak have been taken for comparison.

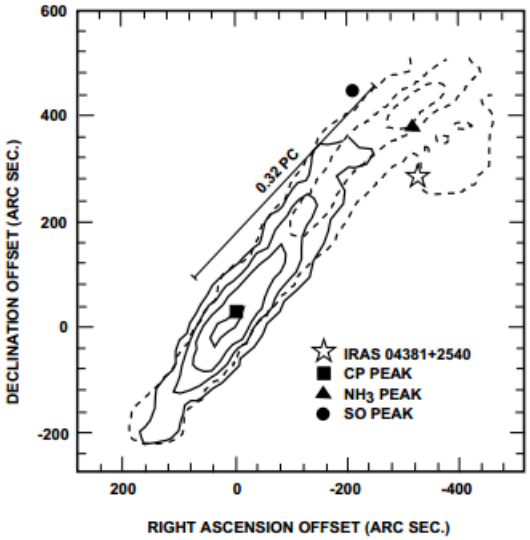

Figure 5.1: Diagram of the TMC-1 ridge ([23]).

5.2 Dating the CP-peak in TMC-1

The temperature has been fixed to 10 K and the visual extinction to 10, closely to what one thinks are the physical parameters of TMC-1. Then, the tools considered to be the keys to study a cloud are applied. From the literature, the range of densities has been constrained to $[10^4 : 10^5$ cm$^{-3}]$. The range of ages is left unchanged : few-10^2 years until few-10^7 years, as in previous sections. Some molecular abundances observed in TMC-1, which are related to this project, are listed in table 5.1.

Provided these values, the chemical clocks are determined : CS/SO = 1.4 and NH_3/HCN = 3 (NH_3/SO = 8.6, NH_3/HCO^+ = 7.1). Both ratios at early and late times agree that TMC-1 should have a chemical age between 10^5 and 3×10^5 years (see figure 5.2) which is consistent with the study of Freeman and Millar, based on the relative abundances of carbon-chain species ([9]). In addition, comparing observations and models allow to note that, in this range of densities, there is no

density-dependence for the observed ratio. Consequently, the assessment of the age is easier and less confusing.

Species	Abundance relative to H_2 [cm^{-3}]	Reference
SO	7(-9)	[47]
CS	1(-8)	[47]
NH_3	6(-8)	[47]
HNC	2(-8)	[48]
HCO^+	8.4(-9)	[23]

Table 5.1: Observed molecular abundances in TMC-1. a(b) means a$\times 10^b$.

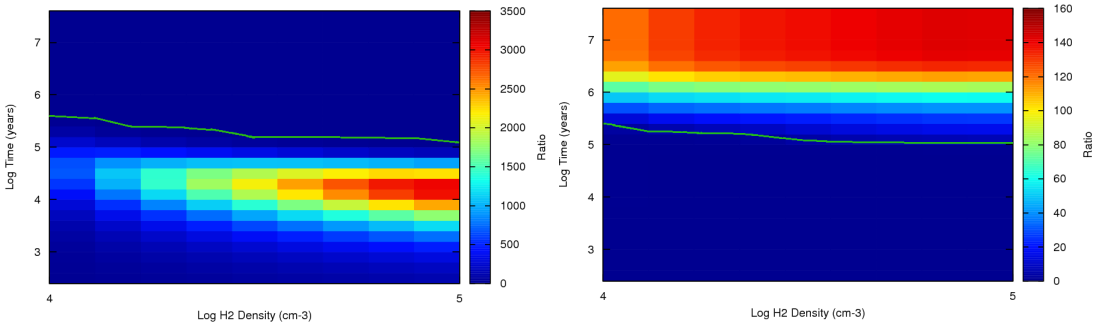

(a) CS/SO. (b) NH_3/HCN.

Figure 5.2: Chemical clocks applied to TMC-1. The green line represents the observational data : 1.4 for CS/SO and 3 for NH_3/HCN.

5.3 Comparison with observational data

In the literature, many observed isotopic ratios for different species are available. But, one has to be careful since (i) some of them, notably the ones where emission lines are weak, have big uncertainties even if not mentioned properly, (ii) depending on the telescope, errors made in measuring abundances, are different.

The ratio of DCO^+ to HCO^+ has been the start point to look at results and propose what seems to be the best model. Subsequently, other ratios have been checked to state whether the initial proposition was right or wrong. Table 5.2 presents the results for some basic and fundamental species. Among all timesteps

which were considered, errors between calculations and observations were minimal for 2×10^5 years (and also 3.2×10^5 years), which is consistent with the previous results. Moreover, a density of 2×10^4 cm^{-3} is found to be the best model for the molecules considered, which is also consistent with what is considered to be the density near the cyanopolyyne peak in TMC-1. The results of all of these calculations lie within a factor of 2 from observations. Though, it is worth noting that ratios concerning C_2H are incoherent with observations. Indeed, even if the CCD over $C^{13}CH$ ratio is consistent with observation, the CCD over ^{13}CCH ratio appears to be similar to the former one. The same phenomena occurs with CCH over ^{13}CCH and $C^{13}CH$. This is against the idea stating that the two isotopomers, $C^{13}CH$ and ^{13}CCH, are distinguishable.

Of course, errors between the model and observations depend strongly on which observational values are chosen. For instance, if one takes the DCN over HCN from Turner ([48]) of 0.01, the error is considerably lowered in table 5.2. Indeed, in some cases, observations lies in quite an extensive range so that it is not straightforward to decide which one is right : they all are, depending on points (i) and (ii) mentioned above. However, when the model does not match observations precisely, it often provides a value which is coherent with this range.

Table 5.2 shows that gas phase and gas grain models give very similar results. It means that, at this particular time, it is too early to see the effects of the freezout onto grains. Indeed, 2×10^5 years is about the time required to see such effects. These similarities are even more pronounced that we talk about ratios where the difference is less stressed than when dealing with direct abundances.

Appendix B lists the relative abundance of selected species and their isotopologues at these optimal parameters.

		Observations	Gas phase only		Gas-grain interactions included	
			Ratio	**Absolute error (%)**	**Ratio**	**Absolute error (%)**
Deuterated ratios	DCO^+	0.015 [29]	0.0162	8	0.02	32
	DNC	0.028 [23]	0.0129	54	0.016	43
	DCN	0.023 [23]	0.0053	77	0.008	64
	N_2D^+	0.08 [23]	0.011	86	0.017	79
	NH_2D	0.01* [23]	0.0095	5	0.015	50
	C_2D	0.01 [29]	0.0088	12	0.0097	3
	HDCS	0.02 [23]	0.031	57	0.035	77
^{12}C to ^{13}C ratios	$H^{13}CN$	56 [48]	103.44	72	90.46	62
	$HN^{13}C$	57.5* [22]	97.86	83	85.39	49
	^{13}CCH	115 [48]	125.47	9	117.26	2
	$C^{13}CH$	58.8 [48]	125.24	53	116.7	50
Other ratios	$DCN/H^{13}CN$	0.59 [48]	0.55	7	0.76	29
	$DNC/HN^{13}C$	1.25 [13]	1.26	1	1.35	8
	$CCD/^{13}CCH$	4.34 [38]	1.11	292	1.14	281
	$CCD/C^{13}CH$	2.24 [38]	1.11	103	1.13	98
	$C^{13}CH/^{13}CCH$	1.6 [38]	1	37	1	37
	$DCO^+/H^{13}CO^+$	0.77 [48]	0.812	5	0.97	26

Table 5.2: Comparison to TMC-1 isotopic ratios for some important species. Best model is obtained at t = 2×10^5 years and n = 2×10^4 cm^{-3}. Relative error (%) = $|\frac{obs-calc}{obs}| \times 100$. The sign * means that the value is an average on different measurements

5.4 The carbon underlying ratio in the CP-peak in TMC-1

Now that the age and the density have been determined, the carbon underlying ratio can be assessed. The cyanopolyyne peak of TMC-1 lies in the range of time (few 10^5 years) where no consensus has been found as for the ratio to be used to predict the ^{12}C to ^{13}C ratio. However, it has been seen that HNC/HN^{13}C might work until 10^5 years and after 10^6 years but not in between as the variations are not weak there, except if the density is high, wich is not the case of TMC-1. Consequently, it is preferable to use the carbon isotope ratio of HCO^+ since it works well for environments older than 10^5 years and this molecule has been observed carefully for decades. Observationally the following ratios are available : $\frac{DCO^+}{HCO^+}$ and $\frac{DCO^+}{H^{13}CO^+}$ (see table 5.2), which lead to $\frac{HCO^+}{H^{13}CO^+} = 51.3$. The $^{12}C/^{13}C$ - Time chromatic plot of the HCO^+ carbon ratio is presented figure 5.3. It allows to assess the carbon underlying ratio at 75 for a density of 2×10^4 cm^{-3}.

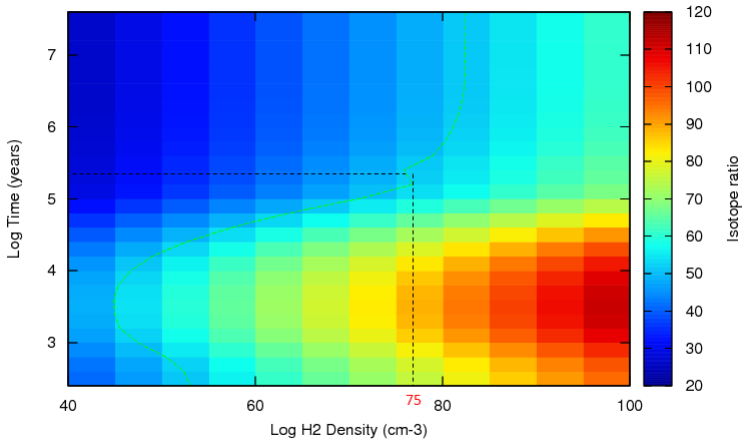

Figure 5.3: $^{12}C/^{13}C$ - Time chromatic plot of the ratio $HCO^+/H^{13}CO^+$ at n = 2×10^4 cm^{-3}. The dotted green line represents the observational value of 51.3.

Chapter 6

Conclusion and future work

6.1 Summary

A chemical network including the main isotopes of carbon (^{12}C, ^{13}C), oxygen (^{16}O, ^{18}O) and hydrogen(H, D) was produced. As much as possible, rules were determined for specific chemical functional groups and for the isotope motions inside or between reactants and products. Adopting statistical branching ratios, attention was also paid to the scale of rate coefficients between "normal" and isotopologic reactions. Along with a previously developed model, this network enables us to study any species and its isotopologues in a specific environment (as density, temperature, cosmic ionisation rate are parameters in the program), at any timestep until 10^8 years.

The upgraded network was first used to predict temporal and density variations over time of the isotopologues of HNCO, which is thought to trace either dense, far infrared or shocked regions. The different isotopologic ratios present strong variations both with density and time, except the carbon one which is more homogeneous around an hypothetical carbon underlying ratio. These results are then compared with some basic molecules containing the main elements, such as CO, HCO^+ and

H_2CO.

In some theoretical studies, observations are either compared with early times models or steady state ones. However, it is obvious that (i) not all astronomical objects have the same age and belong to that particular ranges of time; (ii) the relative abundance of a species varies more or less strongly with time. Consequently, a chemical tool which can constrain the age of an object, could be interesting to understand its chemistry. The abundance ratios CS/SO and NH_3/SO appear to be good chemical clock for early times (t $< 10^5$ years) whereas those of NH_3/HCN (NH_3/HNC) and NH_3/HCO^+ work well for later ages. Indeed, they exhibit large and sudden temporal variations for all densities between 10^3 and 10^7 cm^{-3}. Consequently, even if errors are not minimal, there is less doubt on what model (density, temperature and time fixed) fits the best the observational data.

Furthermore, models always start with a presumed initial chemistry. Especially for isotopes, even if terrestrial underlying ratios are known not to work in the interstellar medium, one has to start with a certain value (different from the terrestrial one) which is also known to be inexact. As a consequence, the project aimed also at finding tools to assign these isotope underlying ratios. The ratios $HNC/HN^{13}C$, $HCO^+/H^{13}CO^+$ and $CH^+/^{13}CH^+$ are interesting. In specific ranges of time and at particular density, they present a barely constant value which can be used to determine the carbon underlying ratio. In addition, extreme precision on the age of the object is not required as the temporal variations are flat.

These tools have been applied to study a particular interstellar cloud : the cyanopolyyne peak of the Taurus Molecular Cloud TMC-1 is found to be around 2 $\times$ 10^5 years years, has a density of about 2 $\times$ 10^4 cm^{-3} and a carbon underlying ratio of 75. These values are consistent with the literature, which suggests that these chemical tools can be applied to other molecular clouds with some confidence.

6.2 Future work

6.2.1 Modelling

Programs made to fractionate the chemical network could be improved in several ways. Indeed, many assumptions have been made which lead to errors in the output provided. For instance, the way a chemical functional group moves and the scale of branching ratios, when including isotopologues, lead to forbidden reactions and/or wrong rate coefficients. Either programs need to be improved to automatically consider and think of every rules to move each functional group or the output file needs to be checked manually, which is really time-consuming.

Furthermore, the way gas grain interactions have been treated is not the best way as it does not follow the species on the grains surface. Instead of modifying the rate coefficients, "new" species should be produced (that is to say, the same as in the gas phase but on grains). This was not a prior goal of the project so it has not been tried. However, it could be interesting if one would like to study more deeply species whose abundance is strongly linked to surface chemistry.

6.2.2 Other chemical tools

In addition of these modelling improvements, the next step would be to look at other association of species to test the underlying isotope ratios and serve as chemical clocks. The chemical network developed and the model provided enable us to study any molecule. It is thus possible to find more useful tools which could work both for early and late times. Indeed, many astronomical objects are between 10^5 and 10^6 years so a unique tool for this range of ages will be convenient.

6.2.3 Observations

This project aimed at providing observers with tools to study a molecular cloud. As a consequence, performing an observational survey on a particular cloud would be a good idea. The first thing is to confirm if the models agree with observations for many isotopologues in the same object. Mainly, this survey would be the occasion to test the predictions for chemical clocks and underlying isotope ratios.

Appendices

Appendix A

Other possible chemical clocks

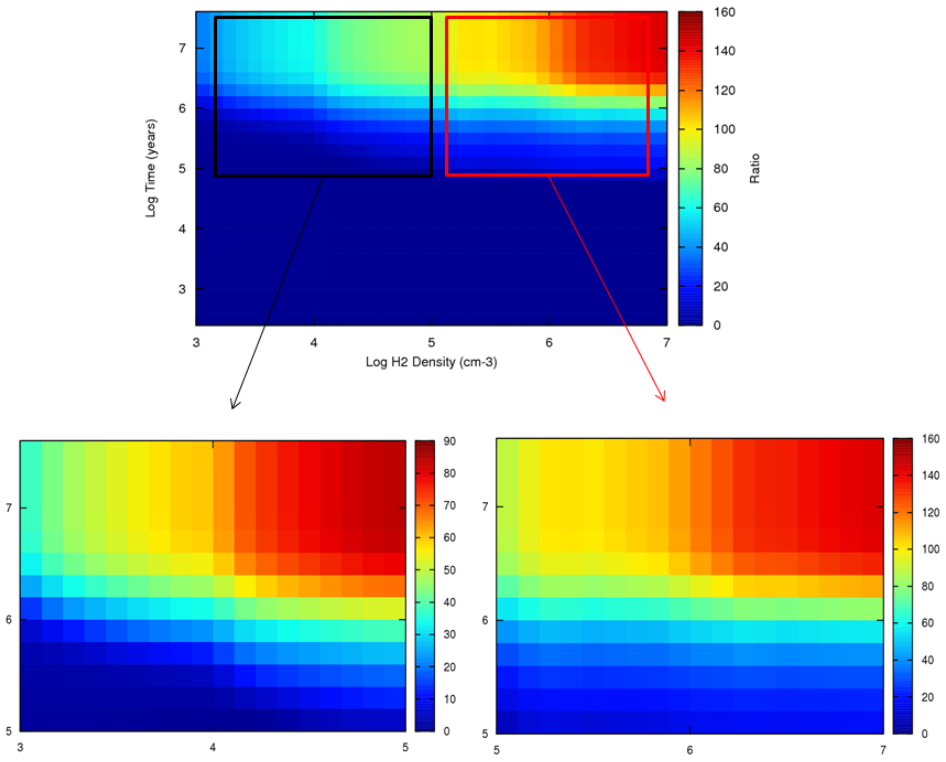

Figure A.1: Density - Time chromatic plots for the NH_3/HNC ratio.

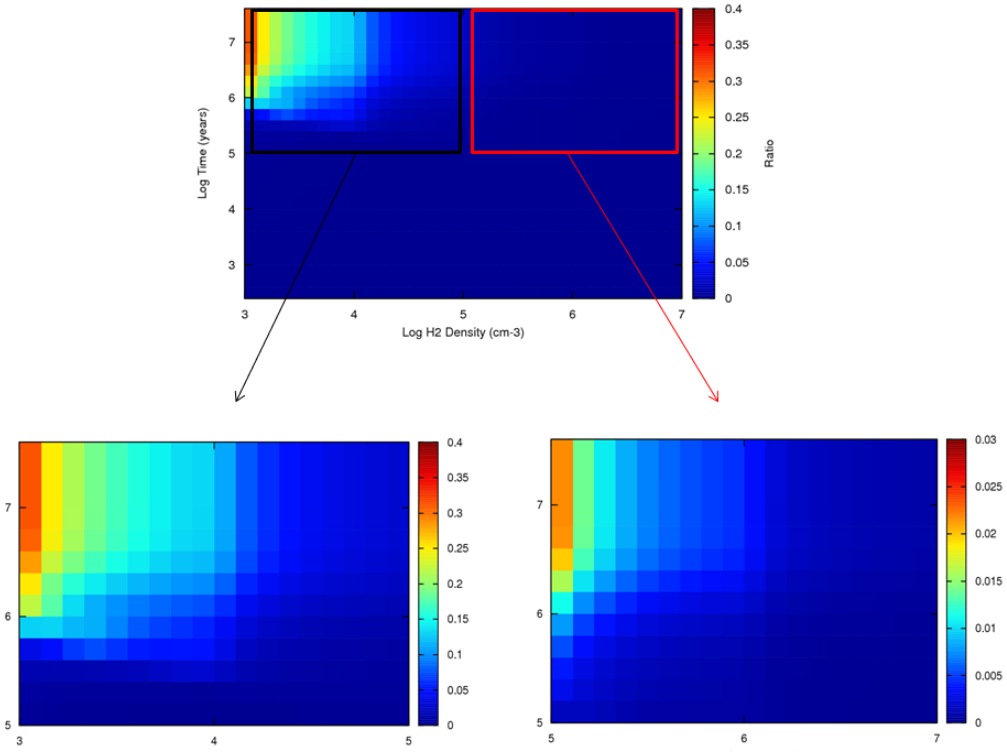

Figure A.2: Density - Time chromatic plots for the N_2H^+/HCN ratio.

Appendix B

Selected species in the modelled TMC-1

Table B.1: Relative abundance of selected species and their isotopologues at 2×10^4 cm^{-3}, 10 K, 2×10^5 years (1).

Species	Abundance	Isotopologues	Abundance
H	4.86(-4)	D	1.699(-6)
H_2	2(+4)	HD	2.814(-5)
H_3^+	3.536(-10)	H_2D^+	1.025(-11)
H_2O	2.858(-7)	HDO	3.097(-9)
		$H_2{}^{18}O$	5.867(-10)
NH_3	2.919(-8)	NH_2D	2.772(-10)
NH_2^+	7.661(-15)	NHD^+	3.311(-18)
CN	8.983(-9)	^{13}CN	1.176(-10)
HCN	4.059(-8)	DCN	2.156(-10)
		$H^{13}CN$	3.924(-10)
HNC	3.62(-8)	DNC	4.671(-10)
		$HN^{13}C$	3.699(-10)

Table B.1: Relative abundance of selected species and their isotopologues at 2×10^4 cm^{-3}, 10 K, 2×10^5 years (2).

Species	Abundance	Isotopologues	Abundance
O_2	3.158(-8)	$O^{18}O$	2.54(-10)
OH	1.465(-8)	OD	9.22(-11)
		^{18}OH	3.001(-11)
CO	2.471(-4)	^{13}CO	3.464(-6)
		$C^{18}O$	4.938(-7)
CO_2	1.126(-6)	$^{13}CO_2$	1.224(-8)
		$CO^{18}O$	4.496(-9)
HCO^+	3.609(-9)	DCO^+	5.851(-11)
		$H^{13}CO^+$	7.206(-11)
		$HC^{18}O^+$	1.328(-11)
H_2CO	2.093(-10)	HDCO	5.302(-12)
		$H_2{}^{13}CO$	2.172(-12)
		$H_2C^{18}O$	4.198(-13)
CH_3OH	2.371(-13)	CH_2DOH	4.651(-15)
		CH_3OD	3.756(-15)
		$^{13}CH_3OH$	2.572(-15)
		$CH_3{}^{18}OH$	4.802(-16)
HNCO	9.939(-12)	DNCO	5.425(-14)
		$HN^{13}CO$	9.338(-14)
		$HNC^{18}O$	1.997(-14)
SO	1.041(-10)	$S^{18}O$	2.132(-13)
SO_2	1.296(-12)	$SO^{18}O$	5.25(-15)
CS	9.142(-9)	^{13}CS	9.058(-11)
H_2CS	1.188(-9)	HDCS	3.723(-11)
		$H_2{}^{13}CS$	1.551(-11)

Bibliography

[1] R. D. Brown and E. Rice. Interstellar deuterium chemistry. *Royal Society of London Philosophical Transactions Series A*, 303:523–533, December 1981.

[2] P. Bruston, J. Audouze, A. Vidal-Madjar, and C. Laurent. Physical and chemical fractionation of deuterium in the interstellar medium. *Astrophysical Journal*, 243:161, January 1981.

[3] J. V. Buckle and G. A. Fuller. Sulphur-bearing species as chemical clocks for low mass protostars? *Astronomy and Astrophysics*, 399:567–581, February 2003.

[4] M. Centurion, C. Cassola, and G. Vladilo. The $^{12}CH^+/^{13}CH^+$ ratio in the Coalsack. *Astronomy and Astrophysics*, 302:243, October 1995.

[5] E. T. Chambers, J. M. Jackson, J. M. Rathborne, and R. Simon. Star formation activity of cores within infrared dark clouds. *Astrophysical Journal, Supplement*, 181:360–390, April 2009.

[6] S. B. Charnley. Sulfuretted molecules in hot cores. *Astrophysical Journal*, 481:396, May 1997.

[7] E. Churchwell, D. Wood, P. C. Myers, and R. V. Myers. The excitation, abundance, and distribution of HNCO in Sagittarius B2. *Astrophysical Journal*, 305:405–416, June 1986.

[8] E. Falgarone, B. Godard, J. Cernicharo, M. de Luca, M. Gerin, T. G. Phillips, J. H. Black, D. C. Lis, T. A. Bell, F. Boulanger, A. Coutens, E. Dartois, P. Encrenaz, T. Giesen, J. R. Goicoechea, P. F. Goldsmith, H. Gupta, C. Gry, P. Hennebelle, E. Herbst, P. Hily-Blant, C. Joblin, M. Kaźmierczak, R. Kołos, J. Krełowski, J. Martin-Pintado, R. Monje, B. Mookerjea, D. A. Neufeld, M. Perault, J. C. Pearson, C. Persson, R. Plume, M. Salez, M. Schmidt, P. Sonnentrucker, J. Stutzki, D. Teyssier, C. Vastel, S. Yu, K. Menten, T. R. Geballe, S. Schlemmer, R. Shipman, A. G. G. M. Tielens, S. Philipp, A. Cros, J. Zmuidzinas, L. A. Samoska, K. Klein, A. Lorenzani, R. Szczerba, I. Péron, P. Cais, P. Gaufre, A. Cros, L. Ravera, P. Morris, S. Lord, and P. Planesas. CH^+(1-0) and $^{13}CH^+$(1-0) absorption lines in the direction of massive star-forming regions. *Astronomy and Astrophysics*, 521:L15, October 2010.

[9] A. Freeman and T. J. Millar. Formation of complex molecules in TMC-1. *Nature*, 301:402–404, February 1983.

[10] R. T. Garrod, S. L. W. Weaver, and E. Herbst. Complex chemistry in star-forming regions: An expanded gas-grain warm-up chemical model. *Astrophysicl Journal*, 682:283–302, July 2008.

[11] M. Guelin, W. D. Langer, and R. W. Wilson. The state of ionization in dense molecular clouds. *Astronomy and Astrophysics*, 107:107–127, March 1982.

[12] J. Hatchell, M. A. Thompson, T. J. Millar, and G. H. MacDonald. Sulphur chemistry and evolution in hot cores. *Astronomy and Astrophysics*, 338:713–722, October 1998.

[13] T. Hirota, M. Ikeda, and S. Yamamoto. Mapping observations of DNC and $HN^{13}C$ in dark cloud cores. *Astrophysical Journal*, 594:859–868, September 2003.

[14] E. Iglesias. The chemical evolution of molecular clouds. *Astrophysical Journal*, 218:697–715, December 1977.

[15] J. M. Jackson, J. T. Armstrong, and A. H. Barrett. HNCO in molecular clouds. *Astrophysical Journal*, 280:608–614, May 1984.

[16] Y.-J. Kuan and L. E. Snyder. Three Millimeter Molecular Line Observations of Sagittarius B2. II. High-Resolution Studies of $C^{18}O$, HNCO, NH_2CHO, and $HCOOCH_3$. *Astrophysical Journal*, 470:981, October 1996.

[17] Sun Kwok. *Physics and Chemistry of the Interstellar Medium*. Sausalito, Calif. : University Science, 2007.

[18] W. D. Langer, P. F. Goldsmith, E. R. Carlson, and R. W. Wilson. Evidence for isotopic fractionation of carbon monoxide in dark clouds. *Astrophysical Journal, Letters*, 235:L39–L44, January 1980.

[19] W. D. Langer, T. E. Graedel, M. A. Frerking, and P. B. Armentrout. Carbon and oxygen isotope fractionation in dense interstellar clouds. *Astrophysical Journal*, 277:581–590, February 1984.

[20] J. L. Linsky, B. T. Draine, H. W. Moos, E. B. Jenkins, B. E. Wood, C. Oliveira, W. P. Blair, S. D. Friedman, C. Gry, D. Knauth, J. W. Kruk, S. Lacour, N. Lehner, S. Redfield, J. M. Shull, G. Sonneborn, and G. M. Williger. What Is the Total Deuterium Abundance in the Local Galactic Disk? *Astrophysical Journal*, 647:1106–1124, August 2006.

[21] H. S. Liszt. Formation, fractionation, and excitation of carbon monoxide in diffuse clouds. *Astronomy and Astrophysics*, 476:291–300, December 2007.

[22] H. S. Liszt and L. M. Ziurys. Carbon isotope fractionation and depletion in TMC1. *Astrophysical Journal*, 747:55, March 2012.

[23] A. J. Markwick, S. B. Charnley, and T. J. Millar. Deuterium fractionation along the TMC-1 ridge. *Astronomy and Astrophysics*, 376:1054–1063, September 2001.

[24] S. Martín, J. Martín-Pintado, and R. Mauersberger. HNCO abundances in galaxies: Tracing the evolutionary state of Starbursts. *Astrophysical Journal*, 694:610–617, March 2009.

[25] S. Martín, M. A. Requena-Torres, J. Martín-Pintado, and R. Mauersberger. Tracing shocks and photodissociation in the Galactic Center Region. *Astrophysical Journal*, 678:245–254, May 2008.

[26] D. McElroy, C. Walsh, A. J. Markwick, M. A. Cordiner, K. Smith, and T. J. Millar. The UMIST database for astrochemistry 2012. *Astronomy and Astrophysics*, 550:A36, February 2013.

[27] A. McKellar. Evidence for the molecular origin of some hitherto unidentified interstellar lines. *Publictions of the ASP*, 52:187, June 1940.

[28] S. N. Milam, C. Savage, M. A. Brewster, L. M. Ziurys, and S. Wyckoff. The $^{12}C/^{13}C$ isotope gradient derived from millimeter transitions of CN: The case for galactic chemical evolution. *Astrophysical Journal*, 634:1126–1132, December 2005.

[29] T. J. Millar, A. Bennett, and E. Herbst. Deuterium fractionation in dense interstellar clouds. *Astrophysical Journal*, 340:906–920, May 1989.

[30] H. W. Moos, K. R. Sembach, A. Vidal-Madjar, D. G. York, S. D. Friedman, G. Hébrard, J. W. Kruk, N. Lehner, M. Lemoine, G. Sonneborn, B. E. Wood, T. B. Ake, M. André, W. P. Blair, P. Chayer, C. Gry, A. K. Dupree, R. Ferlet, P. D. Feldman, J. C. Green, J. C. Howk, J. B. Hutchings, E. B. Jenkins, J. L. Linsky, E. M. Murphy, W. R. Oegerle, C. Oliveira, K. Roth, D. J. Sahnow, B. D. Savage, J. M. Shull, T. M. Tripp, E. J. Weiler, B. Y. Welsh, E. Wilkinson, and B. E. Woodgate. Abundances of Deuterium, Nitrogen, and Oxygen in the Local Interstellar Medium: Overview of First Results from the FUSE Mission. *Astrophysical Journal Supplement Series*, 140:3–17, May 2002.

[31] Nguyen-Q-Rieu, C. Henkel, J. M. Jackson, and R. Mauersberger. Detection of HNCO in external galaxies. *Astronomy and Astrophysics*, 241:L33–L36, January 1991.

[32] K. I. Öberg, C. Qi, D. J. Wilner, and M. R. Hogerheijde. Evidence for multiple pathways to deuterium enhancements in protoplanetary disks. *Astrophysical Journal*, 749:162, April 2012.

[33] C. M. Oliveira, G. Hébrard, J. C. Howk, J. W. Kruk, P. Chayer, and H. W. Moos. Interstellar Deuterium, Nitrogen, and Oxygen Abundances toward GD 246, WD 2331-475, HZ 21, and Lanning 23: Results from the FUSE Mission. *Journal*, 587:235–255, April 2003.

[34] A. A. Penzias. Interstellar HCN, HCO^+, and the galactic deuterium gradient. *Astrophysical Journal*, 228:430–434, March 1979.

[35] A. M. Ritchey, S. R. Federman, and D. L. Lambert. Interstellar CN and CH^+ in diffuse molecular clouds: $^{12}C/^{13}C$ ratios and CN excitation. *Astrophysical Journal*, 728:36, February 2011.

[36] H. Roberts, E. Herbst, and T. J. Millar. Enhanced deuterium fractionation in dense interstellar cores resulting from multiply deuterated H_3^+. *Astrophysical Journal, Letters*, 591:L41–L44, July 2003.

[37] N. J. Rodríguez-Fernández, M. Tafalla, F. Gueth, and R. Bachiller. HNCO enhancement by shocks in the L1157 molecular outflow. *Astronomy and Astrophysics*, 516:A98, June 2010.

[38] N. Sakai, O. Saruwatari, T. Sakai, S. Takano, and S. Yamamoto. Abundance anomaly of the ^{13}C species of CCH. *Astronomy and Astrophysics*, 512:A31, March 2010.

[39] P. Sanhueza, J. M. Jackson, J. B. Foster, G. Garay, A. Silva, and S. C. Finn. Chemistry in infrared dark cloud clumps: A Molecular Line Survey at 3 mm. *Astrophysical Journal*, 756:60, September 2012.

[40] F. Scappini, C. Codella, C. Cecchi-Pestellini, and T. Gatti. The chemical age of the Bok Globule CB238. *Astronomical Journal*, 142:70, September 2011.

[41] Y. Sheffer, M. Rogers, S. R. Federman, D. L. Lambert, and R. Gredel. Hubble Space Telescope Survey of interstellar $^{12}CO/^{13}CO$ in the solar neighborhood. *Astrophysical Journal*, 667:1002–1016, October 2007.

[42] D. Smith and N. G. Adams. Laboratory studies of isotope fractionation in the reactions of C^+ and HCO^+ with CO - interstellar implications. *Astrophysical Journal*, 242:424–431, November 1980.

[43] L. E. Snyder and D. Buhl. Interstellar isocyanic acid. *Astrophysics Journal*, 177:619, November 1972.

[44] S. W. Stahler. The cyanopolyynes as a chemical clock for molecular clouds. *Astrophysical Journal*, 281:209–218, June 1984.

[45] H. Suzuki. Molecular line survey of dark clouds. In M. S. Vardya and S. P. Tarafdar, editors, *Astrochemistry*, volume 120 of *IAU Symposium*, page 199, 1987.

[46] D. M. Tideswell, G. A. Fuller, T. J. Millar, and A. J. Markwick. The abundance of HNCO and its use as a diagnostic of environment. *Astronomy and Astrophyics*, 510:A85, February 2010.

[47] A. Tieftrunk, G. Pineau des Forets, P. Schilke, and C. M. Walmsley. SO and H_2S in low density molecular clouds. *Astronomy and Astrophysics*, 289:579–596, September 1994.

[48] B. E. Turner. Deuterated molecules in translucent and dark clouds. *Astrophysical Journal, Supplement*, 136:579–629, October 2001.

[49] B. E. Turner, R. Terzieva, and E. Herbst. The physics and chemistry of small translucent molecular clouds. XII. More complex species explainable by gas-phase processes. *Astrophysical Journal*, 518:699–732, June 1999.

[50] V. Wakelam, P. Caselli, C. Ceccarelli, E. Herbst, and A. Castets. Resetting chemical clocks of hot cores based on S-bearing molecules. *Astronomy and Astrophysics*, 422:159–169, July 2004.

[51] W. D. Watson, V. G. Anicich, and W. T. Huntress, Jr. Measurement and significance of the equilibrium reaction $^{13}C^+ + {}^{12}CO$ yields $^{12}C^+ + {}^{13}CO$ for alteration of the $^{13}C/^{12}C$ ratio in interstellar molecules. *Astrophysical Journal, Letters*, 205:L165–L168, May 1976.

[52] R. W. Wilson, W. D. Langer, and P. F. Goldsmith. A determination of the carbon and oxygen isotopic ratios in the local interstellar medium. *Astrophysical Journal Letters*, 243:L47–L52, January 1981.

[53] T. L. Wilson. Isotopes in the interstellar medium and circumstellar envelopes. *Reports on Progress in Physics*, 62:143–185, February 1999.

[54] P. M. Woods and K. Willacy. Carbon isotope fractionation in protoplanetary disks. *Astrophysical Journal*, 693:1360–1378, March 2009.

[55] A. Wootten. Deuterated molecules in interstellar clouds. In M. S. Vardya and S. P. Tarafdar, editors, *Astrochemistry*, volume 120 of *IAU Symposium*, pages 311–318, 1987.

[56] I. Zinchenko, C. Henkel, and R. Q. Mao. HNCO in massive galactic dense cores. *Astronomy and Astrophysics*, 361:1079–1094, September 2000.